NACA

# RESEARCH MEMORANDUM

## A METHOD FOR THE DESIGN OF POROUS-WALL WIND TUNNELS

By George M. Stokes

Langley Aeronautical Laboratory
Langley Field, Va.

NATIONAL ADVISORY COMMITTEE
FOR AERONAUTICS

WASHINGTON

January 20, 1956
Declassified July 26, 1957

NATIONAL ADVISORY COMMITTEE FOR AERONAUTICS

RESEARCH MEMORANDUM

# A METHOD FOR THE DESIGN OF POROUS-WALL WIND TUNNELS

By George M. Stokes

## SUMMARY

This report contains a description of a general method for the design of a porous wall (slotted and perforated) wind tunnel which can be applied to the design of low Mach number supersonic wind tunnels. This design method is concerned with the development of a uniform supersonic flow in the wind tunnel and the selection of the proper test-section open ratio necessary to minimize shock-wave-reflection interference. The main feature of the method is its ability to indicate how design requirements and wall porosity characteristics can be combined to achieve a good flow for desired conditions. A limited amount of experimental data has been obtained to show that the method can successfully produce a suitable flow field for model testing. More research is necessary, however, before the practical significance of the method with regard to wave-reflection cancellation can be determined.

The experimental data obtained from a perforated-wall wind tunnel designed by this method showed that the test-section Mach number variation along the center line was ±0.007 for the design Mach number, $M = 1.278$.

A system for calculating the flow in a porous-wall wind tunnel has been developed. This technique is expected to be useful also in determining the flow in the test section at off-design supersonic Mach numbers. When this system was used to calculate the flow in a 3- by 3-inch wind tunnel, it was found that the construction errors in the wall open ratio were sufficiently small to cause no adverse flow variations.

A discussion is included to explain why the open ratio as given by the design method used in selecting the open ratio of the wall does not prevent a disturbance from being generated at the point on the wall where the model shock wave intersects.

## INTRODUCTION

In the interest of developing methods for the design of transonic tunnels having slotted and perforated walls, several different studies

have been made (e.g., refs. 1 and 2). Reference 1, which contains a simplified analysis of the tunnel-wall characteristics required to generate shock-free supersonic flow in minimum distance, indicates that a constant-porosity wall selected on the basis of calibrations with the flow normal to the wall will not generate the desired flow. It does suggest theoretically, however, that a suitable flow distribution could be developed by the use of porous walls if the walls would remove flow at a specified rate at each tunnel station. The study of transonic-wind-tunnel design presented in reference 2 goes a step further in the development of a flow generating method by considering slot discharge coefficients for relating the wall outflow to the slot width. Although in general the principles proposed in these previous design investigations are sound, the work is incomplete to the extent that it does not indicate the influence or treatment of the boundary layer, nor does it show how to determine the required wall-open-ratio distribution to satisfy desired flow conditions.

Since it is important in the cases of shock-wave-reflection studies (refs. 3 and 4) to have a design method available whereby certain desired boundary conditions may be stipulated, further study has been devoted to the development of a porous-wall transonic-design method. The problem was investigated from the points of view of keeping the flow-generation region short, thus obtaining minimum power loss, and of controlling the thickness of the boundary layer at the end of the flow-generation region. The results of this study yielded a successful design method. This report contains a detailed description of the developed method.

The general design method presented herein covers a method or system for finding the open ratio required to minimize the shock-wave reflection for constant boundary-layer growth conditions and a method for obtaining within limits any chosen tunnel-flow distribution for a two-dimensional wind tunnel. To show the effectiveness of the design method, experimental results are presented for a perforated-wall wind tunnel designed by the method.

## SYMBOLS AND DEFINITIONS

| | |
|---|---|
| $a$ | speed of sound in air, ft/sec |
| $C_f$ | effective wall friction coefficient (ref. 3) |
| $H$ | total pressure, lb/sq ft |
| $H_j$ | total pressure in tunnel main stream over porous wall, $H_1$ - Shock losses, lb/sq ft |

| | |
|---|---|
| $h$ | height of tunnel, in. |
| $M$ | Mach number |
| $m_{nt}$ | total mass-flow rate per unit area through porous material, slugs/ft$^2$-sec |
| $m_{nt}'$ | total mass-flow rate per unit area through porous material for $\delta = 0$, slugs/ft$^2$-sec |
| $m_{nbl}$ | mass-flow rate per unit area through porous material required to compensate for boundary-layer growth rate, slugs/ft$^2$-sec |
| $m_{ex}$ | component of stream mass-flow rate normal to center line providing for supersonic expansion, slugs/ft$^2$-sec |
| $P$ | static pressure in stream, lb/sq ft |
| $P_j$ | static pressure in plenum chamber (ref. 5), lb/sq ft |
| $\Delta P$ | static pressure drop across porous material, $P_s - P_j$, lb/sq ft |
| $T$ | temperature |
| $V$ | velocity, ft/sec |
| $V_{nt}$ | component of velocity normal to porous material, $m_{nt}/\rho_s$, ft/sec |
| $V_j$ | jet velocity, velocity corresponding to pressure ratio $P_j/H_j$ across porous material (ref. 5), ft/sec |
| $r$ | open ratio, ratio of open area of porous material to total area of material |
| $w$ | width of wall, in. |
| $\delta$ | stream deflection angle caused by model, or stream angle with respect to tunnel center line ($\delta$ positive for streamlines diverging from center line), deg |
| $\delta^*$ | boundary-layer displacement thickness, in. |
| $d\delta^*/dx$ | rate of change of boundary-layer displacement thickness over wall |

$d\theta/dx$ rate of change of boundary-layer momentum thickness over porous wall

$\rho$ density of gas before entering porous material, slugs/cu ft

$\rho_j$ density of gas in jet (ref. 5), slugs/cu ft

$\rho_{o2}$ stagnation density behind oblique shock

$\nu$ angle through which a supersonic stream is turned to expand from $M = 1$ to $M > 1$ (ref. 6), deg

$\nu_a$ stream expansion angle resulting from flow expansion of the same family or same wall, deg

$\nu_b$ stream expansion angle resulting from expansions of family opposite to that of $\nu_a$, deg

$\sigma$ discharge coefficient for parallel flow, $m_{nt}/\rho_j V_j r$ (see ref. 5)

$\gamma$ porous-wall convergence angle (angle positive with walls converging downstream toward tunnel center line), deg

$\gamma'$ ratio of specific heat of gas at constant pressure to specific heat at constant volume

Subscripts:

o stagnation conditions

1 free-stream conditions in test section

2 conditions behind oblique shock caused by model

ah ahead

j nonviscous jet conditions with plenum-chamber static pressure (ref. 5) and stream total pressure

bl boundary layer

p porous wall

max maximum

pt point

s stream condition

sw solid wall

The word "porous" is considered throughout the paper to apply to both perforated and slotted materials.

The words "plenum chamber" are used herein to denote the low-pressure chamber on the opposite side of the porous wall from the test section.

## GENERAL DESIGN METHOD

The general design method has been developed to apply to two-dimensional wind tunnels having porous top and bottom walls and solid side walls. (See fig. 1.) As shown in this figure, the porous walls are vented into a plenum chamber which is attached to a suction supply. The upstream portion of the porous material is used for generating the required supersonic flow by means of expansion associated with outflow into the plenum chamber. The remaining porous material is used to form the walls of the test section.

In the design of transonic tunnels, it is necessary to consider the wall interference effects resulting from reflecting disturbances as well as the uniform requirements of the test section. Because of this the general design method is presented in two parts; one part shows how to determine the open ratio needed in the test section to minimize the shock reflections, and the other shows how to determine a wall-open-ratio distribution in the flow-generation region which will give a uniform flow in the test section. Since an important consideration is given to the boundary-layer growth by the design method, a brief description of the boundary-layer behavior with respect to porous materials will be presented first.

### Estimation of Boundary-Layer Growth

Only a little published information appears to be available (refs. 3 and 7) to show how the boundary layer grows over porous materials or what the friction coefficients for such materials might be. Recently, however, a limited number of tests were made in the Langley 3- by 3-inch transonic flow apparatus to determine the boundary-layer growth rates over a 41-percent-open porous specimen. The test specimen was a $2\frac{1}{4}$- inch-square perforated sheet 0.060 inch thick, having 0.0407-inch-diameter holes.

Pressure measurements were made to determine the thickness of the boundary layer at two points; one point was 1/8 inch upstream of the specimen and the other was 1/8 inch downstream of the specimen. From these data, the boundary-layer growth rate $d\delta^*/dx_p$ was found by dividing the difference between the downstream and upstream boundary-layer-displacement thickness by $2\frac{1}{4}$ inches. The results of the tests are shown in figures 2, 3, and 4.

The data of these three figures were taken with the upstream boundary-layer displacement thickness, $\delta^*$, equal to approximately 0.002 inch, and with the stagnation constants $H_o$ and $T_o$ equal to 30 inches of mercury and 200° F, respectively. Figure 2 shows how the boundary-layer growth rate $d\delta^*/dx_p$ changes with the outflow velocity ratio $V_{nt}/V_s$ for several values of the free-stream Mach number. These data are presented in this form to expedite their use with the design method. Curves describing the boundary-layer growth relationship should be obtained for a range of open ratios to define completely the growth rate with respect to the open ratio. Thus, the data presented in figure 2 are inadequate for determining accurately the boundary-layer growth rates over similar specimens at different open ratios, and for other upstream boundary-layer thicknesses. Nevertheless, if some approximate calculation is desired, it is believed that these data may be used for estimating the boundary-layer growth rates for open ratios within 10 to 20 percent of the measured value of open ratio. One method used for making these estimates is to assume (1) that a linear relationship exists between the open ratio and the rate of growth of the boundary layer at zero outflow and (2) that the rate-of-growth curves for other open ratios would have approximately the same shape as a function of outflow velocity ratio $V_{nt}/V_s$ as the curves for the 41-percent-open material. By use of these assumptions, the data of figure 2, and a solid-wall boundary-layer growth rate of 0.002 (ref. 3), the boundary-layer growth rate over a 20-percent-open perforated plate would be estimated to be 0.004 for a zero outflow velocity condition at a Mach number of 1.01. To estimate the total boundary-layer growth rate in wind tunnels having both solid and porous walls, the boundary-layer growth of the solid wall must be added to that of the porous walls. The following expression shows how these two boundary-layer growth conditions enter the porous-wall outflow equation:

$$m_{nt} = \rho_s V_{nt}$$

$$= \rho_s V_s \sin(\delta + \gamma) + \rho_s V_s \frac{d\delta^*}{dx_p} \cos(\delta + \gamma) + \rho_s V_s \frac{h_{sw}}{w_p} \frac{d\delta^*}{dx_{sw}} \cos \gamma \quad (1)$$

This equation was obtained by assuming the flow conditions pictured in the sketch below.

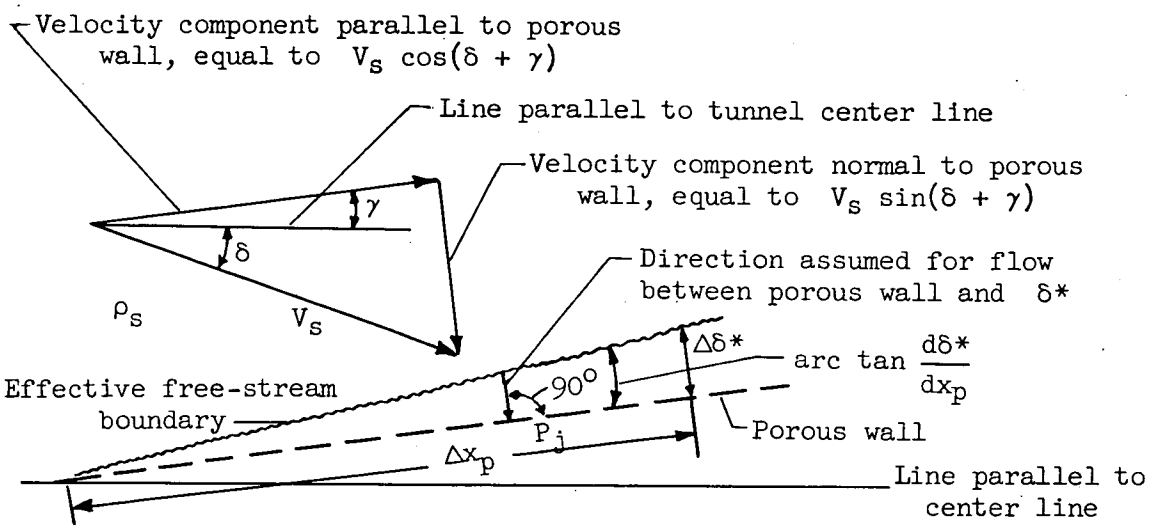


The term $\rho_s V_s \sin(\delta + \gamma)$ of equation (1) denotes the mass rate of outflow through the porous wall resulting from the flow angle $\delta$ and the wall convergence $\gamma$. The terms $\rho_s V_s \frac{d\delta^*}{dx_p} \cos(\delta + \gamma)$ and $\rho_s V_s \frac{h_{sw}}{w_p} \frac{d\delta^*}{dx_{sw}} \cos \gamma$ of equation (1) represent the additional mass rate of outflow taken through the porous wall to account for the boundary-layer growth over the porous walls and side walls, respectively. In the development of equation (1), it was assumed that the flow crossing the effective free-stream boundary over the porous wall turned in a direction normal to the wall and passed through. This consideration is equivalent to assuming that a void exists between the effective free-stream boundary and the wall. The last term of equation (1), representing the mass rate of flow through the porous wall needed to compensate for the increase of boundary-layer displacement thickness over the side wall is an approximation, since in general the flow angle on the side walls is different from zero and variable over the wall height $h_{sw}$. For convenience, the sum of the boundary-layer growth terms $\rho_s V_s \frac{d\delta^*}{dx_p} \cos(\delta + \gamma)$ and $\rho_s V_s \frac{h_{sw}}{w_p} \frac{d\delta^*}{dx_{sw}} \cos \gamma$ will be denoted as $m_{nbl}$. For the condition of uniform flow in the wind tunnel (i.e., $\delta = 0$), equation (1) becomes

$$m_{nt}' = \rho_s V_s \left( \tan \gamma + \frac{d\delta^*}{dx_p} + \frac{h_{sw}}{w_p} \frac{d\delta^*}{dx_{sw}} \right) \cos \gamma \qquad (2)$$

It should be noted that the solution of equation (1) for $m_{nt}$ cannot be obtained directly. This results because the boundary-layer growth rate over the porous portion of a wind tunnel is a function of the total outflow $m_{nt}$ and also of $V_{nt}/V_s$. If all the terms of equation (1) are known except the term containing $d\delta^*/dx_p$, a solution of the equation can be found by an iteration process. This may be accomplished by first assuming $\frac{d\delta^*}{dx_p} = 0$ and then finding the value of the $V_{nt}/V_s$ given by the other terms of equation (1). This value of $V_{nt}/V_s$ is used to determine (from curves for the particular material similar to those of fig. 2) an approximate value of $d\delta^*/dx_p$ to be tried in the next calculation for $V_{nt}/V_s$. This iteration process is repeated until the value of $V_{nt}/V_s$ resulting from equation (1) is equal to the value used to read $d\delta^*/dx_p$. The value of $m_{nt}$ obtained by use of this converged value of $d\delta^*/dx_p$ is the required result.

When using the data presented in figure 2, it should be remembered that the boundary-layer growth over a perforated material depends not only upon the velocity ratio $V_{nt}/V_s$ and Mach number, but also upon other flow variables. This can be shown if the following form of the momentum equation

$$\frac{d\theta}{dx} + \frac{\theta}{M}\frac{dM}{dx}\left[\frac{(2 - M^2) + H'}{1 + \frac{\gamma' - 1}{2}M^2}\right] - \frac{\rho_s V_{nt}}{\rho_s V_s} = \frac{C_f}{2}$$

is rewritten in terms of boundary-layer displacement thickness. This gives

$$\frac{d\delta^*}{dx_p} = \frac{\delta^*}{H'}\frac{dH'}{dx} - \frac{\delta^*}{M}\frac{dM}{dx}\left[\frac{(2 - M^2) + H'}{1 + \frac{\gamma' - 1}{2}M}\right] + H'\left[\frac{\rho_s V_{nt}}{\rho_s V_s} + \frac{C_f}{2}\right]$$

where $H'$ is the ratio of the boundary-layer displacement thickness to the momentum thickness and $\gamma'$ is the ratio of the gas specific heat at constant pressure to the specific heat at constant volume. Here, it is seen that the boundary-layer growth is a function of the displacement thickness, the form factor $H'$, the stream Mach number and velocity, the porous wall outflow velocity, the wall friction, $dM/dx$, and $dH'/dx$.

The most significant point to be made from the data of figure 2 is that the boundary-layer growth rate drops rapidly as the porous-wall

outflow velocity is increased and that the stream Mach number has an appreciable effect on the growth rate.

Figure 3 shows how the effective friction coefficient (for uniform flow) $\frac{C_f}{2} = \frac{d\theta}{dx_p} + \frac{\rho_s V_n}{\rho_s V_s}$ (eq. (3) of ref. 3) varies with outflow velocity and Mach number. The data are presented primarily to show the approximate magnitudes of the friction coefficients for perforated material. Curves of this type are not generally needed when data are available which show the growth of the boundary layer. In addition to the boundary-layer data taken for the 41-percent-open specimen, the porosity characteristics of the material were also measured. The curves of figure 4 show the relationship between discharge coefficient $\sigma$ and velocity ratio $V_s/V_j$ for several Mach numbers. The dashed portions of the curves for the Mach numbers of 1.17 and 1.27 have been extrapolated from the basic data shown. This extrapolation was necessary in order that the range of the data would be sufficiently large for use in the design of the perforated-wall wind tunnel described later in the paper.

## Method for Selecting the Test-Section Wall-Open Ratio

It is well known that shock-wave reflections from wind-tunnel walls in the transonic speed range are quite troublesome. Presently, much research is being conducted toward the development of porous walls in an attempt to reduce the effects of wave reflection. The method presented in this section deals with the selection of the porous-wall open ratio needed in the wind-tunnel test section to reduce or minimize the shock-wave reflecting ability of the tunnel walls.

The method is based on the reasoning that the porous-wall boundary of the wind tunnel will not reflect a model shock-wave disturbance in the stream if the normal component of the stream flow is absorbed by the wall; that is, the flow approaching the wall must be completely removed at its incoming rate. Thus, the problem is one of determining the wall-open ratio necessary to fulfill this condition.

An equation developed in reference 5 is

$$r = \frac{m_{nt}}{\rho_j V_j \sigma} \tag{3}$$

This equation shows how the wall-open ratio is related to the wall outflow, the theoretical jet conditions $\rho_j$ and $V_j$, and the wall porosity characteristic $\sigma$. Equation (3) is used in combination with equation (1) to calculate a value of open ratio for the walls of the test section.

Equation (1) is rewritten for use in this section as

$$m_{nt2} = \rho_2 V_2 \left[ \sin\left(\delta_2 + \gamma\right) + \frac{d\delta^*}{dx_p} \cos\left(\delta_2 + \gamma\right) + \frac{h_{sw}}{w_p} \frac{d\delta^*}{dx_{sw}} \cos \gamma \right] \qquad (4)$$

because the conditions (subscript 2) downstream of an oblique shock are being considered. Similarly, the quantities $\rho_j$, $V_j$, and $m_{nt}$ in equation (3) are defined as $\rho_{j2}$, $V_{j2}$, and $m_{nt2}$ when used to refer to the conditions downstream of the oblique shock.

When solving equations (3) and (4) to find the test-section open ratio it must be assumed (1) that a uniform supersonic flow enters the test section, (2) that the porosity characteristics of the wall type intended for use have been defined similarly to those of figure 4, (3) that the side-wall boundary-layer growth rate is known, (4) that boundary-layer growth rate data similar to those of figure 2 are available, and (5) that the wall convergence angle has been chosen. Equation (4) should first be solved for $m_{nt2}$ for several arbitrarily chosen values of $\delta$ which correspond to values expected at the walls of the tunnel when tests are being conducted.

The values of $r$ which will result from insertion of these values of $m_{nt2}$ in equation (3), will show that a slightly different value of $r$ is obtained when $\delta$ is changed, thus the value of $r$ to be chosen, should be a value which corresponds to a value of $\delta$ that best represents the range of deflection angles expected during wind-tunnel tests. The values of $\rho_{j2}$ and $V_{j2}$ to be used in equation (3) must result from use of a value of the plenum-chamber pressure required to provide a uniform flow in the test section for the value of test-section open ratio which is being determined. Since in equation (3) the quantities $\rho_{j2}$, $V_{j2}$, $r$, and $m_{nt2}$ $\left(\text{because of } d\delta^*/dx_p\right)$ are dependent variables, the solution of the equation must be obtained by use of a cut-and-try process.

Because of the indirect method which must be used to obtain the test-section wall open ratio and because of the complexities involved in solving equations (1) and (3), a detailed step-by-step procedure is introduced here to expand upon the summary solution of the problem just stated and to indicate a practical solution. This procedure is as follows:

1. Choose the desired test-section Mach number, $M_1$. (The chosen Mach number is expected to be in the supersonic range $M = 1.00$ to $M = 1.50$.) Also stipulate the tunnel stagnation conditions $H_{o1}$ and $T_{o1}$, and the convergence angle $\gamma$.

2. Determine from oblique shock theory (ref. 6), the stream conditions $H_2/H_{o1}$, $\rho_2/\rho_{o1}$, $a_2/a_{o1}$, $\rho_{o2}/\rho_{o1}$, and $M_2$ downstream of the shock wave for several values of $\delta_2$ from 0 to $\delta_2 = \delta_{2max}$. It is advisable to plot these quantities versus $\delta_2$. This will account for all values of strengths of the weak shock which may be encountered in supersonic flow up to $\delta_{2max}$. Expansion waves are not accounted for by this design method.

3. For the stagnation conditions of step 1, and by the use of reference 6, compute $H_2$, $\rho_2$, $V_2$, and $\rho_{o2}$ for the range of $\delta_2$'s chosen in step 2.

4. Neglect the boundary-layer terms and the convergence angle $\gamma$ in equation (4) for the present and determine the resulting values of $m_{nt2}$ given by

$$m_{nt2} = \rho_2 V_2 \sin \delta_2$$

to obtain approximate values of the required test-section mass-outflow rates. Use the values of $\rho_2$ and $V_2$ from step 3 for the range of $\delta_2$ in step 2.

5. Neglect the boundary-layer growth in the test section ahead of the shock and the wall convergence angle $\gamma$ so that $P_1 = P_j$. Also take the total pressure $H_{j2} = H_2$ and compute $P_j/H_{j2}$, for the range of $\delta_2$'s in step 2.

6. From the pressure ratios $P_j/H_{j2}$ obtained in step 5, calculate by use of reference 6 the corresponding values of $\rho_{j2}$ and $V_{j2}$ (assuming isentropic flow) using the relations $\rho_{j2} = \frac{\rho_{j2}}{\rho_{oj2}} \rho_{oj2}$, $V_{j2} = M_{j2} \frac{a_{j2}}{a_{oj2}} a_{oj2}$ where $\rho_{oj2} = \rho_{o2}$ and $a_{oj2} = a_{o1} = \gamma' R T_{o1}$.

7. The quantity $\sigma$ needed in the evaluation of equation (3) must be determined from curves showing the porosity characteristics of the wall type for use. If no such data are available, it will be necessary to determine $\sigma$ experimentally for a sample of material having a value of open ratio guessed to be in the range required. The data of reference 5, which show some curves of $\sigma$ plotted against $V_s/V_j$, indicate that it is not essential to make the calibrations for determining $\sigma$ for the exact open ratio of the material required in the final configuration.

8. By use of $m_{nt2}$ of step 4, $\rho_{j2}$ and $V_{j2}$ of step 6, and values of $\sigma$ for $V_2/V_j$ for the corresponding $M_2$, calculate using equation (3), the approximate values of open ratio required for the range of $\delta_2$'s chosen in step 2.

9. Select from the open-ratio values obtained in step 8 a value of open ratio which corresponds to a flow deflection angle, $\delta_2$, which best represents the range expected during wind-tunnel tests, and determine from experiments on a sample of material having this value of open ratio curves of $d\delta^*/dx_p$ as a function of $V_{nt}/V_s$ for several values of $M$ (in the range of $M_2$). Also determine curves of $\sigma$ similar to those of figure 4 for this material to check the values previously used.

10. Start with this step to recalculate the values of open ratio required in the test section for various values of $\delta_2$ with the tunnel boundary layer included. Estimate $d\delta^*/dx_{sw}$ by use of the momentum equation in conjunction with reference 8, or by use of experimental measurements.

11. Using the curves obtained in step 9 and the $d\delta^*/dx_{sw}$ estimated in step 10, obtain $m_{nt}'$ (by the iteration procedure previously discussed in conjunction with eqs. (1) and (2)) for the region of parallel flow in the test section upstream of the shock. Also obtain the values of $m_{nt2}$ for the range of $\delta_2$ in step 2, including the boundary-layer terms and the convergence angle $\gamma$ in equation (4).

12. In order to find the plenum-chamber pressure with the boundary layer included in the calculation, proceed by the use of reference 6, and find $M_{j1}$, $\rho_{j1}/\rho_{oj1}$, and $a_{j1}/a_{oj1}$ for a chosen range of pressure ratios $P_j/H_{j1}$, slightly less than the pressure ratio value given by $P_1/H_{o1}$, and calculate values of

$$m_{nt1} = \sigma r \rho_{j1} V_{j1} = \sigma r \frac{\rho_{j1}}{\rho_{oj1}} \rho_{o1} M_{j1} \frac{a_{j1}}{a_{oj1}} a_{o1}$$

(where $\rho_{oj1} = \rho_{o1}$ and $a_{oj1} = a_{o1}$) for this range of pressure ratios using the $r$ selected in step 9.

13. Compute $P_j = \frac{P_j}{H_{j1}} H_{o1}$ (where $H_{j1} = H_{o1}$) for the values $P_j'/H_{j1}$ chosen in step 12 and plot $P_j$ as a function of the corresponding values of $m_{nt1}$ determined in step 12. Read a value of $P_j$ from this curve

for a value $m_{nt1}$ equal to the value of $m_{nt}'$ determined in step 11. This gives the plenum-chamber static pressure required to provide uniform flow in the empty test section.

14. Using the $P_j$ determined in step 13 and $H_{j2} = H_2$, recalculate $P_j/H_{j2}$ and the corresponding values of $\rho_{j2}$ and $V_{j2}$, as in step 6.

15. Make new calculations for r (eq. (3)) using the values $m_{nt2}$ from step 11, with the corresponding values of $\rho_{j2}$ and $V_{j2}$ from step 14, and the curves $\sigma$ as in step 8 for the range of $\delta$'s considered.

The newly calculated required open-ratio range resulting from the inclusion of the boundary-layer growth will in most cases indicate that a test-section open ratio different from the one estimated in step 9 (no boundary layer) is needed. Thus, several iterations (using steps 9 to 15) may be required before the final open-ratio selection made is equal to the value used for estimating the boundary-layer growth and finding $P_j$.

The above method has been found to be effective in determining analytically the required open ratio of a porous wall. It must be borne in mind, however, that as indicated, the method accounts for only one boundary-layer growth rate along the wall behind an oblique shock for a given $\delta$ and $\gamma$; thus, if the growth rate changes appreciably with distance for different downstream stations through this region, a constant value of open ratio in the test section will not provide the necessary outflow.

## Flow Generation

This section describes a method for designing a porous supersonic wind-tunnel nozzle capable of providing a uniform supersonic flow at a chosen Mach number in a given distance. It is assumed when using this method that a uniform sonic flow will enter a two-dimensional supersonic flow-generation section of the tunnel, and that the walls providing the flow expansion will be porous and will be surrounded by a plenum chamber in which the pressure can be controlled. The schematic drawing in figure 1 pictures a representative tunnel configuration.

To initiate the design of the nozzle, certain quantities must be chosen; these are the test-section Mach number, the tunnel stagnation pressure and temperature, the test-section open ratio r, the rate of supersonic flow expansion for $\nu_a$ family, the convergence angle, the physical dimensions of the tunnel, and the side-wall boundary-layer growth rate $d\delta^*/dx_{sw}$. With this information and a requirement that the porous wall originate at the minimum area or point where M = 1.0, a two-dimensional supersonic characteristic net (ref. 9) must be constructed

for the chosen expansion rate, or center-line Mach number distribution, to obtain a theoretically desired flow for the flow-generation section of the tunnel. From this characteristics network, the flow quantities $\rho_s$, $V_s$, $\delta$, and $M$ for various stations along the porous wall can be calculated by use of the given set of tunnel stagnation conditions and the isentropic flow tables (ref. 6).

To determine the distribution of the wall-open ratio, $r$, required to provide these desired flow conditions equations (1) and (3) are again available; that is,

$$m_{nt} = \rho_s V_s \left[ \sin(\delta + \gamma) + \frac{d\delta^*}{dx_p} \cos(\delta + \gamma) + \frac{h_{sw}}{w_p} \frac{d\delta^*}{dx_{sw}} \cos \gamma \right]$$

and

$$r = \frac{m_{nt}}{\rho_j V_j \sigma}$$

The values of $\rho_s$, $V_s$, and $\delta$ to be used in equation (1) are those determined from the Mach net at the position of the wall in conjunction with the stagnation conditions, $H_{ol}$ and $T_{ol}$. With the use of the above quantities and the given constants of the tunnel, an approximate solution of equation (1) can be determined by use of the method of iteration indicated in the previous section "Estimation of Boundary-Layer Growth," for finding values of $d\delta^*/dx_p$ with assumed values of wall-open ratio. Of course, a solution of equation (1) must be made for many points in the flow-generation region in order adequately to define the mass-outflow rate along the wall.

In equation (3) the values of $\rho_{jl}$ and $V_{jl}$ are related to the plenum-chamber pressure $P_j$ (the value necessary to provide a uniform test section) as in step 13 of the preceding section. Also, in this case $H_{jl} = H_{ol}$ and $T_{oj} = T_{ol}$. The quantity $\sigma$ for use in equation (3) is determined as mentioned earlier by use of curves of $\sigma$ plotted against $V_s/V_j$ as functions of $M$ for the material. Approximate values of $r$ can now be calculated from the approximate mass-outflow quantities $m_{nt}$. The values of $r$ obtained at this point are only approximate values because only assumed or guessed values of $r$ were considered in the solution of $m_{nt}$. Thus, an iteration involving $r$ as well as $V_{nt}/V_s$ must be used as in the preceding section to determine $m_{nt}$. The final value of $r$ is determined by using the approximate values obtained from succeeding calculations in performing the next, until the degree of

convergence desired is reached. This procedure is used to determine the distribution of $r$ for the flow-generation section of the tunnel.

Since the pressure $P_j$ in the plenum chamber outside the porous walls will normally be constant over the length of the nozzle and test section and since the stagnation conditions $H_{o1}$ and $T_{o1}$ for the flow in the nozzle are constant, $\rho_j$ and $V_j$ are constant (and equal to $\rho_{j1}$, $V_{j1}$) for any particular nozzle design.

In the foregoing method, it was assumed that the open ratio of the test section was determined by the method presented in the section entitled "Selection of the Test-Section Wall Open Ratio." Insofar as the design of the flow generation is concerned, any value of $r$ (within reasonable limits) could be chosen for the test section. A different choice in the test section $r$ would simply require a different plenum chamber $P_j$ necessary to provide uniform flow in the test section. From this pressure $P_j$ new values of $\rho_j$ and $V_j$, for use in equation (3), would be determined.

Although the flow-generation design method is rigorous in principle, it is possible to make serious errors in a tunnel design if the boundary-layer growth rates are not known with reasonable accuracy. A nozzle flow calculation which will be presented in a later section may be used to examine the accuracy to which these quantities must be known.

## APPLICATION OF THE DESIGN METHOD

In order to evaluate experimentally the effectiveness of the previously discussed design method, an approximately 3- by 3-inch two-dimensional supersonic porous-wall wind tunnel was designed, constructed, and tested. The results determined from using the method for selecting the test-section wall-open ratio will be given first and will be followed by a description of how the "Flow-Generation Design Method" was used in the design of the nozzle.

It was pointed out in the section entitled "General Design Method" that certain design constants or quantities must be chosen; those chosen for the design of this approximately 3- by 3-inch wind tunnel are as follows:

| | |
|---|---|
| $M_1$ | 1.278 |
| $T_o$, $^oF$ | 200 |
| $H_o$, lb/sq ft | 2086.54 (= 29.50 in. Hg) |

| | |
|---|---|
| Initial family, $\nu_a$, supersonic flow expansion rate, deg/in. | 1.86 |
| Tunnel height, in. | 2.954 |
| Tunnel width, in. | 3.018 |
| $\gamma$, deg | 0 |
| Side walls | Solid and parallel |
| Top and bottom porous walls | Flat and parallel |

The reasons for choosing these particular constants were (1) so that the supersonic nozzle and test section resulting from this particular design could be tested in an available test apparatus and (2) so that the tunnel Mach number and flow angles resulting from proposed model tests would be in a range in which other data were available for comparison. Because the boundary-layer growth-rate curves of figure 2 had not been determined at the time this tunnel design was made and because no other thorough system was known for estimating the wind-tunnel boundary-layer growth, a departure from the general design method was made to obtain a quantity for $m_{nbl}$ to represent the boundary-layer growth mass-flow rate.

The quantity $m_{nbl} = 0.008$ was chosen to represent the mass-outflow rate required in the test section for both the glass side walls and the perforated wall. The value of $m_{nbl} = 0.008$ was derived partially through the use of some experimental data of $m_{nbl}$ from tests made in a tunnel having 18-percent-open perforated walls, and partially by a guess as to how the boundary-layer might grow over a wall with an increasing value of open ratio.

## Calculation of Test-Section Wall-Open Ratio

With the exception of the determination of the boundary-layer growth mass-flow rate the design method given in the section on "Method for Selecting the Test-Section Wall-Open Ratio" was used for calculating the open ratio for the test section of the approximately 3-inch-square tunnel.

The quantities $M_2$, $H_2/H_{o1}$, $\rho_{o2}$, $H_2$, $\rho_{o2}$, $\rho_2$, and $V_2$ for the 3-inch-square tunnel were determined for the range of $\delta_2$'s given in table I. The values found for $M_2$, $H_2/H_{o1}$, $\rho_2$, and $V_2$ have been listed in table I.

The quantities $\rho_{j2}$ and $V_{j2}$ used in equation (3) were found by first using an approximate value of $P_j\left(= P_1\right)$ to obtain approximate values of $\rho_{j2}$ and $V_{j2}$ for computing approximate values of $r$ for the range of $\delta_2$'s in table I. From these data a value of $r = 0.47$ appeared best to represent values of $\delta_2$ between $2^\circ$ and $3^\circ$.

Next the range of $P_j/H_j$ values in table II were assumed. The calculations in table II for $P_j$, $\rho_{j1}$, $V_{j1}$, and $m_{nt}$ were then made with use of the value of $r = 0.47$. Examination of the data of table II showed $m_{nt} = 0.00799$ when $\frac{P_j}{H_{j1}} = 0.369$. Since this quantity of 0.00799 was approximately equal to $m_{nbl} = 0.008$ the $P_j$ for the tunnel was 769.87 pounds per square foot. The values of $\rho_{j2}$ and $V_{j2}$ for the range of $\delta_2$ were next computed. The curves of figure 4 were used to determine values of $\sigma$.

Since a constant value of $m_{nbl} = 0.008$ was assumed for all values of $\delta_2$ no iterative solution was required to determine $m_{nt2}$ from equation (1). Table I shows the values determined for $m_{nt2}$. The values of $V_2/V_j$, $\sigma$, and $r$ (shown in table I) were then found for the range of $\delta_2$'s chosen. The results of these calculations showed that a value of $r = 0.47$ should be a reasonable average for use in the test section.

Since the method described for selecting the test-section wall open ratio indicates that the boundary layer should be estimated by the use of curves similar to those of figure 2, calculations were made to find what values of wall-open ratio would result when using this system. Table III shows some of the quantities used in making these calculations. Notice that the values of the open ratio given in table III are not appreciably different from those of table I for values of $\delta_2 = 2.57^\circ$ or above. This approximate duplication occurs because the boundary-layer growth estimates used for the two cases form only a small percentage of the total wall outflow. The greatest influence of the boundary-layer growth occurs at the low values of $\delta_2$.

The open-ratio values given in tables I and III for $\delta_2 = 0$ can be used as an index to show what values of open ratio were used in the iteration solution to find the other values of $r$ in the table. Remember the value of $r$ assumed to find $P_j$ ($\delta_2 = 0$) should, in the final solution, be approximately equal to the $r$ selected for the test section.

Although the total pressure losses across an oblique shock wave are included in the calculation of tables I and III, no appreciable errors would have been caused if these shock losses were neglected. If the data of table III had been used in selecting the test-section open ratio, a value of $r$ slightly lower than 0.47 would have been chosen. A sample calculation is given in appendix A to show how the boundary layer was estimated for table III.

## Design of Nozzle

According to the method as stated in the section on flow generation, a supersonic characteristic flow net was constructed for a 1.86° per inch first family $\nu_a$ expansion rate (ref. 9). The characteristic net was completely contained between parallel boundaries $h/2$ apart, and the characteristic lines were initiated at the boundary (chosen to represent the porous wall) for each $\frac{1.86^\circ}{4}$ $\nu_a$ family expansion. All characteristics intersecting the wall boundary from the family $\nu_b$ were assumed to have no downstream wall reflection, and thus, were terminated at the wall intersection point. This type of construction will result in the development of a network which will yield a parallel flow in the minimum distance. With the nozzle characteristic network complete, it was possible to determine the flow expansion angles along the tunnel walls. Table IV shows the expansion angles determined for the design of the approximately 3-inch-square wind tunnel. These expansion angles were used to compute $\delta_s = (\nu_a - \nu_b)$, $M_s$, $\rho_s$, and $V_s$, at each chosen wall station for the given tunnel stagnation conditions.

It was pointed out in the "Flow Generation" section, that equations (1) and (3) should be used to calculate the required open ratio $r$ of the wall, for wall-flow conditions, as determined for the characteristic network, and for the values of $\rho_{j1}$ and $V_{j1}$ as determined from the conditions of the empty test section. This procedure was followed in the design of this nozzle with the exception that the boundary-layer growth terms were evaluated differently. The reason for making the change in estimating the boundary layer has been explained earlier. The boundary-layer mass-flow rate distribution term, $m_{nbl}$, in this design was estimated by first neglecting boundary-layer growth in the flow generation region and computing an $r$ distribution with the use of equations (1) and (3). The values of $\rho_{j1}$ and $V_{j1}$ used in the calculation were the values determined in the previous section "Selection of the Test-Section Open Ratio" using a test section $m_{nbl} = 0.008$, $\delta_2 = 0$, and $r = 0.47$.

Examination of the resulting $r$ distribution showed that the tunnel-open ratio increased rapidly with increasing downstream distance until the nozzle station 1.5 inches downstream of the entrance of the flow-generation region was reached. At this station, the nozzle open ratio was approximately that of the test section; from this point on, the open-ratio distribution became nearly constant throughout the remainder of the flow-generation region until the last few stations were reached. These data led to the boundary-layer mass-flow estimates $m_{nbl}$ given in table IV. The boundary-layer growth mass flow $m_{nbl}$ was assumed to increase linearly with distance (from 0 to 0.008) until the 1.5-inch

station was reached, and then to remain constant for the following downstream stations. This approximation of the boundary-layer growth estimate was added to the outflow necessary for supersonic expansion to give the total outflow rate $m_{nt}$ at the various tunnel stations. These data and the porosity characteristics $\sigma$ taken from data of figure 4 were inserted into equation (3) to compute the required open-ratio distribution of the tunnel. The results of the calculations are tabulated in table IV. A sample calculation for this table is given in appendix B. The flow-generation region of the nozzle ends at station 3.79. The open ratio for all stations downstream of this point must be the preselected test-section open-ratio value, 0.47.

## Construction and Tests

The wall-open-ratio distribution for the wind tunnel was achieved by drilling two 0.060-inch-thick aluminum-alloy plates with holes ranging in diameter from 0.016 inch to 0.046 inch. Figure 5 shows a photograph of one of the walls. The holes were drilled in rows across the tunnel width, with all holes in each row having the same diameter. The rows were spaced approximately 0.030 inch apart. Each row was drilled so that the total open area required for a 0.030 by 3.018 strip would be given by the holes. Although considerable care was taken in the drilling of the walls, the final wall-open-ratio distribution as determined by measurements was slightly different, in general, from that computed in the design. The data of figure 6 show a comparison between the measured and design open-ratio values. In order to show what these construction errors mean in percent of open ratio, the data of figure 7 are given.

When the measured values of open ratio (fig. 6) were used to compute the flow field of the nozzle, the data of figure 8 were obtained. (The system used in calculating the nozzle flow, with the wall-open ratio given, will be explained later.) If the data of figure 7 are used in conjunction with the data of figure 8, it is possible to note at some points the effect of errors in wall construction on the flow generation. For instance, the 11-percent error in wall-open ratio at station 0.51 can be seen to cause a rapid change in Mach number occurring at station 0.51 of figure 8(a). This error introduced at station 0.51 also affects the flow at the center-line station 1.2 and the wall station 2.1 as shown in figures 8(b) and 8(a), respectively. The next downstream center-line station which could have been affected by the disturbance resulting from this upstream open-ratio error is station 3.21. Notice, however, that no appreciable flow disturbance shows up at this point. This result is believed to occur because the turning angle provided by the wall at station 2.1 on account of the presence of the disturbance itself is of the correct magnitude and direction to cancel the incoming disturbance. Since the downstream flow is influenced by errors in open ratio made upstream, it is difficult to establish from the data of figure 8, the exact effect of an open-ratio error at a given station.

Nevertheless, it can be stated that the open ratios as measured for the porous wall are sufficiently small to provide an approximately uniform center-line flow downstream of station 2.6.

When the tunnel was put into operation, center-line pressure measurements were taken to determine the degree of flow uniformity. The data of figure 9 show the Mach number variations through the nozzle and test section for three different settings of plenum-chamber pressure. On this figure, the circles represent the experimental data for the design condition (M = 1.278), and the solid line indicates the designed Mach number distribution. The experimental data show that the flow expansion in the nozzle started at least 0.2 inch upstream of station zero. This upstream expansion, which is quite common in both perforated- and slotted-wall nozzles, is believed to be due to a decrease in the boundary-layer thickness as the perforated portion of the nozzle is approached.

The general overexpansion occurring at the center line in the downstream portion of the flow-generation region (stations 1 to 2.6) is probably caused by the use of an inaccurate boundary-layer growth rate in the design. The assumption made in design that $m_{nbl}$ in the flow-generation region increases linearly from 0 at station zero to 0.008 at station 1.5 was probably considerably in error because (1) figure 2 shows that $d\delta^*/dx_p$ decreases as $V_{nt}/V_s$ increases; thus the actual $\rho_s V_s \frac{d\delta^*}{dx_p}$ term would decrease at first with increasing station in the nozzle and be quite small for the high wall outflow rates; and (2) the boundary-layer growth on the side walls is approximately constant and becomes the governing component of $m_{nbl}$ when $\rho_s V_s \frac{d\delta^*}{dx_p}$ is small.

The walls were designed to be flat between the wall stations zero and 11.5. Surface measurements, however, revealed that wall waves of ±0.003 inch existed on each wall. The exact effects of these surface contours on the flow could not be definitely determined; however, these wall variations must have influenced the flow to some degree.

The experimental data taken at Mach numbers 1.1 and 1.2 (fig. 9) are included to show the type of flow distribution which was obtained at off-design Mach numbers. A comparison of these data with those taken at the design Mach number shows that much more severe flow variation occurred at the off-design Mach numbers.

Insofar as the testing of models is concerned, the flow variations in this 3- by 3-inch tunnel are sufficiently small to provide a suitable test region. For example, at the design Mach number (M = 1.278), the maximum Mach number variation along the center line between the stations 2.5 and 12.0 is $\Delta M = \pm 0.007$. The rapid flow generation, which

was achieved in less than one tunnel height, and the extended run of fairly uniform flow, are most encouraging in view of some of the uncertainties involved in estimating the boundary-layer growth, and of the physical precision of the fabricated wall.

## Calculation of a Wind-Tunnel Flow Field

As an outgrowth of some of the principles used in the nozzle design described in this paper, an effective method has been employed for calculating the wind-tunnel flow field. This method primarily involves the finding of the flow conditions at points along the wall and using these flow conditions to determine the wind-tunnel flow field. The discussion given here will cover only the method for finding the flow conditions at one station along a porous wall. Procedures are already established for determining the stream flow once the flow at the boundary is known (ref. 9).

To determine the values of $M$ and $\delta$ at a given point on the wall, it is necessary to know the flow conditions just upstream of the point to be computed. This requirement will in general, make it necessary to start the calculations at the tunnel minimum, where the flow is uniform and $M = 1.0$. It is also necessary to specify the wall boundary-layer growth, the wall convergence, wall-porosity characteristics $\sigma$ and open ratio, and plenum-chamber pressure. With these quantities given and with the aid of equations (1) and (3), the flow removal rate through the porous wall at any station providing for supersonic expansion in a tunnel can be found by solving the following expression:

$$m_{ex} = \rho_{jl} V_{jl} r\sigma - m_{nbl} = m_{nt} - m_{nbl} = \rho_s V_s \sin(\delta + \gamma) \tag{5}$$

For the special case of parallel walls, equation (5) becomes:

$$m_{ex} = \rho_{jl} V_{jl} r\sigma - m_{nbl} = \rho_s V_s \sin \delta \tag{6}$$

To determine the Mach number resulting from this outflow, first find the flow angle $\delta_{pt}$ at the point. This flow angle may be used in conjunction with the upstream flow conditions of $\delta_{ah}$ and $\nu_{ah}$ to find the expansion angle at the point. The following equation shows how these quantities are related:

$$\nu_{pt} = \nu_{ah} + \left(\delta_{pt} - \delta_{ah}\right) \tag{7}$$

The Mach number can be determined from the expansion angle $\nu_{pt}$.

An examination of the variables in equation (5), rewritten in the form

$$\rho_s V_s \sin(\delta + \gamma) = \rho_{j1} V_{j1} r\sigma - \rho_s V_s \frac{d\delta^*}{dx_p} \cos(\delta + \gamma) + \frac{h_{sw}}{w_p} \frac{d\delta^*}{dx_{sw}} \cos\gamma \qquad (8)$$

shows that to determine the value of $\delta$ at a point from this equation, it is necessary to know the Mach number at the point because the quantities $\rho_s V_s$, $d\delta^*/dx_p$, and $\sigma$ are functions of M. Since M is one of the wall quantities to be found from the final solution, equations (5) and (7) must be solved by an iteration process. If, in solving for the outflow or $\delta_{pt}$, the stream quantities $\rho$, V, M, $d\delta^*/dx_p$, and $\sigma$ just upstream of this point are used for the values of $\rho$, V, M, $d\delta^*/dx_p$, and $\sigma$ at the point, these quantities will serve as a good first approximation for the iteration. The Mach number determined from this first calculation of $\nu_{pt}$ may now be used for making the second approximation, and the results of the second in computing the third, etc. A more rapid convergence for the iteration will occur, however, if the average value of Mach number resulting from the two next preceding approximate calculations is used for recomputing $M_{pt}$ and $\delta_{pt}$. The most important use for this wind-tunnel flow-field calculating system is that it makes possible calculations of the stream flow conditions at any off-design Mach number, and thus should be useful to one who wishes to design a transonic tunnel to operate over a range of Mach numbers.

The circles shown in figure 8 are calculated for the 3- by 3-inch tunnel by use of the design specification and the measured open-ratio distribution. These data were determined by calculating the flow field produced by each lateral row of holes. The average row spacing was 0.03015 inch. Normally, only three iterations were required to satisfy the conditions at the wall to a Mach number accuracy of ±0.00004. The Bell Telephone Laboratory X-66744 relay computing machines were used to make these calculations. For the reader's convenience, a sample calculation of the data of figure 8(a) has been included in appendix C.

## Discussion of the Wave-Reflection Problem

Since a design method has been given for calculating the open ratio needed in a porous-walled test section to minimize shock-wave reflection ability of the wall, some discussion is in order to indicate the phenomena which can be encountered during the practical use of such walls.

In the design method, it was assumed that the boundary-layer growth rate in front of the shock wave would be constant (in test-section region).

It was also assumed that the boundary-layer growth rate would be constant for a given value of $\delta_2$ behind the oblique shock wave. Although these assumptions were necessary to simplify the design problem, it was known that these conditions did not exist in practical wind tunnels. For instance, the boundary-layer thickness over a porous wall was found in reference 3 to change rapidly in the vicinity of the oblique shock wave. The variation in boundary-layer thickness upstream (from shock) resulted because the increased pressure behind the shock traveled upstream through the boundary layer. (Ref. 10 shows this phenomenon occurring over solid walls.) The effect of this pressure behind the shock causes the upstream boundary layer to grow and reach a peak thickness just ahead of the model shock-intersection point and results in the generation of a compression region which in some cases generates a shock in the stream. Immediately downstream of this point, the boundary layer thins because of the pressure rise occurring across the model shock. The thinning of the boundary layer increases the effective area ratio of the tunnel and thus creates an expansion wave. The strength of the expansion is magnified to some extent at this point by the porous walls because of the ability of the wall to remove flow from the tunnel.

It is believed that if the boundary layer over the walls of the tunnel is made thin, as is possible by designing the tunnel to have a value of $\gamma$ much greater than $\arctan \frac{d\delta^*}{dx_p}$, the effect of the boundary layer on the wave reflection of the model shock would be much less severe and would induce only minor flow variation in the stream.

It should also be recognized that, if the boundary-layer growth rates were known in the vicinity of the point where a given strength model shock wave intersects the wall, equations (1) and (3) could be used, theoretically, to calculate a distribution of open ratio along the wall in vicinity of the shock which would eliminate the reflection of the shock. Since this solution for the wave-reflection problem accounts for only one flow condition in the tunnel it appears to be impractical for use in wind-tunnel testing. More research will be required before practical solution to the wave-reflection problem can be demonstrated.

## CONCLUSIONS

The following conclusions summarize the wind-tunnel-design method and experimental information described in this report:

1. An effective method is presented for the design of transonic porous-wall wind tunnels which at present is known to be capable of providing a flow suitable for testing at the design Mach number.

2. The design method permits a supersonic tunnel to be designed to have, within limits, any arbitrarily selected rate of flow expansion in the nozzle or any desired center-line Mach number distribution.

3. Flow generation for a design Mach number of 1.278 can be achieved in less than one tunnel height with test-section Mach number variations within ±0.007.

4. A method is given for calculating the open ratio of the wall needed to maintain a constant pressure field behind an oblique shock wave.

5. The constant value of open ratio in the test section, even though chosen by the design method, is not expected to prevent shock-wave-reflection disturbances in the presence of any appreciable wall boundary layer.

6. Model shock-wave reflections from walls having thin boundary layers are expected to be quite weak when the open ratio of the test section has been chosen through the use of the design method.

7. The quality of the design depends to a considerable degree on how accurately the boundary-layer growth rates over the wall and the porosity characteristics of the porous wall have been determined.

8. The wind-tunnel flow field in a porous-wall tunnel can be determined for any transonic Mach number by the specific calculation procedure given in this report.

Langley Aeronautical Laboratory,
National Advisory Committee for Aeronautics,
Langley Field, Va., October 6, 1955.

# APPENDIX A

## BOUNDARY-LAYER ESTIMATION

In order to illustrate how the boundary-layer growth was estimated in table III, the following calculations were made for $\delta_2 = 0$ (the uniform flow condition in the test section):

Constants given for the design of the 3- by 3-inch tunnel are as follows:

$M_1 = 1.278$

$H_{o1} = 2,086.54$

$T_{o1} = 200^\circ$ F

$\rho_{o1} = 0.0018434$

$\gamma = 0^\circ$

$a_{o1} = 1,261$

$\rho_1 = 0.000909$

$V_1 = 1,399.2$

Boundary-layer growth-rate curves, figure 2

Porosity-characteristic curves, figure 4

Height of solid side walls, 2.954 in.

Width of perforated walls (top and bottom), 3.018 in.

Boundary-layer growth of side walls, $\frac{d\delta^*}{dx_{sw}} = 0.002$

The following assumptions were made:

1. Assume that the boundary-layer-growth curve for $M = 1.22$ in figure 2 applies for the perforated wall at $M = 1.278$.

2. Assume that the required test-section open ratio will be 0.47. (The results of table I indicated that this value should serve as a good first approximation.)

3. Assume as in the section on "Estimation of Boundary-Layer Growth" that the quantity 0.47/0.41 times the boundary-layer growth rate for 41-percent open material gives the boundary-layer growth rate for a 47-percent open wall.

To find the boundary-layer growth mass flow, we must find a solution for equation (4)

$$m_{nt2} = \rho_2 V_2 \sin(\delta_2 + \gamma) + \rho_2 V_2 \left( \frac{d\delta^* \cos(\delta_2 + \gamma)}{dx_p} + \frac{h_{sw}}{w_p} \frac{d\delta^* \cos \gamma}{dx_{sw}} \right)$$

For parallel walls and free-stream conditions in the test section ($\delta = 0^\circ$), $\rho_2 V_2 = \rho_1 V_1$. Therefore,

$$m_{nt1} = \rho_1 V_1 \left( \sin 0^\circ + \frac{d\delta^*}{dx_p} + \frac{h_{sw}}{w_p} \frac{d\delta^*}{dx_{sw}} \right)$$

In order to evaluate the quantity $d\delta^*/dx_p$, an iteration must be used.

To start the solution, first assume $\frac{d\delta^*}{dx_p} = 0$ and $\frac{d\delta^*}{dx_{sw}} = 0.002$ then

$$(m_{nt1})_1 = 0.000909 \times 1399.2 \left( 0 + 0 + \frac{2.954}{3.018} 0.002 \right) = 0.00249$$

Subscripts numbers outside parenthesis denote the number of the iteration step.

$$(V_{nt1})_1 = \frac{(m_{nt1})_1}{\rho_1} = \frac{0.00249}{0.000909} = 2.74$$

$$\frac{(V_{nt1})_1}{V_1} = \frac{2.74}{1399.2} = 0.00196$$

This is the outflow-velocity ratio required to compensate for boundary-layer growth on the side walls.

Now by using $\frac{(V_{ntl})_1}{V_1} = 0.00196$ and the curves of figure 2, the first approximate value of $d\delta^*/dx_p$ will be found to be

$$\frac{d\delta^*}{dx_p} = 0.00625 \times \frac{0.47}{0.41} = 0.007165$$

$$\rho_1 V_1 \frac{d\delta^*}{dx_p} = 0.009113$$

With this term evaluated, the second approximation to the total mass-outflow quantity is

$$(m_{ntl})_2 = (0 + 0.009113 + 0.00249) = 0.11603$$

and the velocity ratio

$$\frac{(V_{ntl})_2}{V_1} = \frac{12.76}{1399.2} = 0.00912$$

Since $(V_{ntl})_2/V_1$ does not equal $(V_{ntl})_1/V_1$ another choice of outflow velocity must be tried. For rapid convergence, one-half the previous value of $\rho_1 V_1 \frac{d\delta^*}{dx_p}$ or $\frac{0.009113}{2}$ is applied for a third approximation

$$(m_{ntl})_3 = 0.004557 + 0.00249 = 0.007047$$

$$= \frac{(V_{ntl})_3}{V_1} = \frac{7.753}{1399.2} = 0.00555$$

for $(V_{ntl})_3/V_1$,

$$\frac{d\delta^*}{dx_p} = 0.00292 \times \frac{0.47}{0.41} = 0.00335$$

$$\rho_1 V_1 \frac{d\delta^*}{dx_p} = 0.004257$$

$$(m_{ntl})_4 = 0.004257 + 0.00249 = 0.006747$$

$$\frac{(V_{ntl})_4}{V_1} = \frac{7.42}{1399.2} = 0.00531$$

for $(V_{ntl})_4/V_1$,

$$\frac{d\delta^*}{dx_p} = 0.00310 \times \frac{0.47}{0.41} = 0.00355$$

$$\frac{(V_{ntl})_5}{V_1} = \frac{7.65}{1399.2} = 0.00547$$

The desired value of $d\delta^*/dx_p$ must fall between the values of $\frac{d\delta^*}{dx_p} = 0.00355$ and 0.00335. By using the average of these two values for a more rapid convergence

$$\frac{d\delta^*}{dx_p} = \frac{0.00355 + 0.00335}{2} = 0.00345$$

$$\frac{(V_{ntl})_6}{V_1} = \frac{7.56}{1399.2} = 0.0054$$

for $(V_{ntl})_6/V_1$,

$$\frac{d\delta^*}{dx_p} = 0.00301 \times \frac{0.47}{0.41} = 0.00345$$

Since the value of $\frac{d\delta^*}{dx_p} = 0.00345$ is the same value as that used in the preceding step, this quantity 0.00345 slug/ft$^2$-sec represents the boundary-layer growth rate over the perforated walls in the test section.

## APPENDIX B

## DETERMINATION OF OPEN RATIO IN NOZZLE

A sample calculation has been prepared to show how to find the open ratio for a station along the wall in the flow-generation region (table IV). By using the constants listed in section "Application of the Design Method" and proceeding as indicated below, the quantities in table IV for the station 1.2 were found.

The values of $\nu_a$ and $\nu_b$ in table IV were read from curves which were determined from the nozzle characteristic flow network.

At the wall station 1.2,

$$\nu_a = 2.233^\circ \quad \text{and} \quad \nu_b = 0.269^\circ$$

$$\nu_s = 2.233 + 0.269 = 2.502^\circ$$

$$\delta_s = 2.233 - 0.269 = 1.964^\circ$$

From the isentropic-flow tables, the value of M for $\nu = 2.502$ is $M = 1.1553$. For this Mach number, the following stream quantities were determined by use of the constants $H_{o1} = 29.50$ in. Hg(= 2,086.5 lb/ft$^2$), and $T_{o1} = 200^\circ$ F:

$$\rho_{o1} = \frac{H_{o1}}{RT_{o1}} = \frac{2086.5}{1715 \times (200 + 460)} = 0.0018434$$

$$a_{o1} = 49.1\sqrt{T_o} = 49.1\sqrt{200 + 460} = 1{,}261 \text{ ft/sec}$$

$$a_s = 1{,}120.3 \text{ ft/sec} \quad \text{for} \quad M = 1.1553$$

$$V_s = M_s a_s = 1.1553 \times 1120.3 = 1{,}294.3 \text{ ft/sec}$$

The quantities $\rho_{j1}$ and $V_{j1}$ to be used in the following equation, equation (3) of the text,

$$r = \frac{m_{nt}}{\rho_j V_j \sigma}$$

are the values determined for $\delta_2 = 0$ in table I. These values are $\rho_{j1} = 0.000904$ and $V_{j1} = 1403.8$. Now having determined the value of $V_{j1}$, the quantity $V_s/V_j$ for the station 1.2 of table IV is found to be

$$\frac{V_s}{V_{j1}} = \frac{1294.3}{1403.8} = 0.9220$$

By use of the curves of figure 4, the value of $\sigma$ corresponding to the stream Mach number ($M = 1.1553$) and velocity ratio $V_s/V_j = 0.9220$ was found to be 0.1370.

The total wall mass-outflow rate $m_{nt}$ is obtained by the use of equation (1) with the exception of the terms including the boundary-layer growth. The mass-outflow rate $m_{nbl}$ necessary to compensate for the boundary-layer growth was found by the system stated in the section entitled "Application of the Design Method," where $m_{nbl}$ was assumed to vary linearly from a value of zero at station zero to a value of 0.008 at station 1.5. Thus, the quantity $m_{nbl} = \frac{0.008 \times 1.2}{1.5} = 0.0064$.

Now to obtain from equation (1) the outflow component providing for supersonic expansion

$$m_{ex} = \rho_s V_s (\sin \delta) \text{ for parallel walls}$$

$$\frac{\rho_s}{\rho_{o1}} = 0.6510 \quad \text{for} \quad M_s = 1.1553$$

$$\rho_s = \frac{\rho_s}{\rho_{o1}} \rho_{o1} = 0.6510 \times 0.0018434 = 0.00102$$

Thus, the value of the supersonic expansion mass outflow is

$$m_{ex} = 0.00102 \times 1120.3 \sin 1.964^\circ = 0.04524$$

and

$$m_{nt} = m_{nbl} + m_{ex} = 0.0064 + 0.04524 = 0.05162$$

therefore,

$$r = \frac{m_{nt}}{\rho_{j1} V_{j1} \sigma} = \frac{0.05162}{0.000904 \times 1403.8 \times 0.1370} = 0.2968 \text{ or } 29.68 \text{ percent}$$

This value of $r = 29.68$ percent is the open ratio the wall must have to satisfy the desired flow conditions at the 1.2-inch station.

## APPENDIX C

## DETERMINATION OF LOCAL MACH NUMBER AND FLOW ANGLE AT A POINT ON THE WALL

In order to find the Mach number and flow angle at a given wall station in the nozzle of the 3- by 3-inch tunnel constructed by the presented design method, the following sample calculation is made:

Given quantities:

$M = 1.0$ upstream of point to be calculated

$\nu_s = 0^\circ$ upstream of point to be calculated

$\delta_s = 0^\circ$ upstream of point to be calculated

$\rho_{0l} = 0.0018434$

$\gamma = 0^\circ$

$T_{0l} = 200^\circ$ F

Station = 0.03015 in. (station for which this calculation is made)

$m_{nbl}$ = 0.00016 slug/ft$^2$-sec (estimated by system described in the section "Design of Nozzle")

$V_{jl} = 1403.8$ (from table IV)

$\rho_{jl} = 0.000904$ (from table IV)

Porosity-characteristic curves of figure 4

Wall-open ratio curves of figure 6 ($r$ at station 0.03015 in. is 0.0047)

The Mach number at the given station, 0.03015, may be determined by finding the solution of equations (5) and (7) at this point. Equation (5) is given as

$$m_{ex} = \left(\rho_{jl} V_{jl} r\sigma - m_{nbl}\right) = \rho_s V_s \sin(\delta + \gamma)$$

for the case where $\gamma = 0$ equation (5) may be rewritten as

$$m_{ex} = \rho_{j1} V_{j1} r\sigma - m_{nbl} = \rho_s V_s \sin \delta$$

and equation (7) is given as

$$\nu_{pt} = \nu_{ah} + \left(\delta_{pt} - \delta_{ah}\right)$$

The unknown quantities which will be determined are $\sigma$, $\rho_s$, $V_s$, and $\delta$.

As was explained earlier $\sigma$, $\rho_s$, and $V_s$ are all functions of the Mach number or $\nu_{pt}$, the quantity which is to be determined; thus, the solution must be found by the use of an iteration process.

To do this, first assume that the velocity at the station being calculated will be the same as that at the upstream station and find the Mach number resulting from this solution. By the use of this upstream point,

$$V_s = M_s \frac{a_s}{a_o} a_o = 1150.3 \text{ (for } M = 1.00)$$

$$\frac{V_s}{V_{j1}} = \frac{1150.3}{1403.8} = 0.820$$

$$\sigma = 0.279$$

Then,

$$m_{ex} = 0.000904 \times 1403.8 \times 0.0047 \times 0.279 - 0.000160 = 0.001504$$

$$\rho_s = \frac{\rho_s}{\rho_{o1}} \rho_{o1} = 0.6339 \times 0.0018434 = 0.001169 \text{ (for } M = 1.000)$$

$$\delta = \delta_{pt_1} = \text{arc sin} \frac{m_{ex}}{\rho_s V_s} = \text{arc sin} \frac{0.001504}{0.001169 \times 1150.3} = 0.06409^\circ$$

The subscript $pt_1$ is being used to denote the first partial results at the point for which the solution is sought. With increasing iteration steps, the partial results will be denoted by $pt_2$, $pt_3$, etc.

$$\nu_{pt_1} = \nu_{ah} + \left(\delta_{pt} - \delta_{ah}\right) = 0 + (0.0641 - 0) = 0.0641^\circ$$

The Mach number resulting from $\nu_{pt_1}$ (M = 1.013) is used to make the following second approximation:

for $M_{pt_1}$:

$$V_s = M_{pt_1} a_{pt_1} = 1.013 \times 0.9110 \times 1261 = 1163.7$$

$$\frac{V_s}{V_{j1}} = \frac{1163.7}{1403.8} = 0.8290$$

$$\sigma = 0.2675$$

$$m_{ex} = (0.000904 \times 1403.8 \times 0.0047 \times 0.2675) - 0.00016 = 0.001435$$

for $M_{pt_1}$:

$$\rho_s = 0.001155$$

$$\delta_{pt_2} = \text{arc sin } \frac{0.001435}{1163.7 \times 0.001155} = 0.06106^\circ$$

$$\nu_{pt_2} = 0 + (0.6106 - 0) = 0.06106^\circ$$

$$M_{pt_2} = 1.01250$$

Similarly the third approximation:

for $M_{pt_2}$:

$$V_s = M_{pt_2} a_{pt_2} = 1.0125 \times 0.9111 \times 1261 = 1163.3$$

$$\frac{V_s}{V_{j1}} = \frac{1163.3}{1403.8} = 0.8286$$

$\sigma = 0.268$

$m_{ex} = (0.000904 \times 1403.8 \times 0.0047 \times 0.268) - 0.000160 = 0.001438$

for $M_{pt_2}$:

$$\rho_s = \frac{\rho_s}{\rho_{o1}} \rho_{o1} = 0.001156$$

$$\delta_{pt_3} = \text{arc sin} \frac{0.001438}{1163.3 \times 0.001156} = 0.06112^\circ$$

$$\nu_{pt_3} = 0 + (0.06112 - 0) = 0.06112^\circ$$

$$M_{pt_3} = 1.01252$$

The value of $M_{pt_3}$ gives the Mach number at station 0.03015 to an accuracy of $\pm 0.00002$.

## REFERENCES

1. Nelson, William J., and Klevatt, Paul L.: Preliminary Investigation of Constant-Geometry, Variable Mach Number, Supersonic Tunnel With Porous Walls. NACA RM L50B01, 1950.

2. Osborne, James I., and Zeck, Howard: Progress Report on Development of a Transonic Test Section for the Boeing Wind Tunnel (BWT 188). Vol. I - December 1950 to June 1951. Doc. No. D-11955, Boeing Airplane Co., Sept. 1951.

3. Davis, Don D., Sellers, Thomas B., and Stokes, George M.: An Experimental Investigation of the Transonic-Flow-Generation and Shock-Wave-Reflection Characteristics of a Two-Dimensional Wind Tunnel With 17-Percent-Open Perforated Walls. NACA RM L54B15a, 1954.

4. Sellers, Thomas B., Davis, Don D., and Stokes, George M.: An Experimental Investigation of the Transonic-Flow-Generation and Shock-Wave-Reflection Characteristics of a Two-Dimensional Wind Tunnel With 24-Percent-Open, Deep, Multislotted Walls. NACA RM L53J28, 1953.

5. Stokes, George M., Davis, Don D., Jr., and Sellers, Thomas B.: An Experimental Study of Porosity Characteristics of Perforated Materials in Normal and Parallel Flow. NACA TN 3085, 1954. (Supersedes NACA RM L53H07, 1953.)

6. Ames Research Staff: Equations, Tables, and Charts for Compressible Flow. NACA Rep. 1135, 1953. (Supersedes NACA TN 1428.)

7. Dorrance, William H., and Dore, Frank J.: The Effect of Mass Transfer on the Compressible Turbulent Boundary-Layer Skin Friction and Heat Transfer. Jour. Aero. Sci., vol. 21, no. 6, June 1954, pp. 404-410.

8. Tucker, Maurice: Approximate Turbulent Boundary-Layer Development in Plane Compressible Flow Along Thermally Insulated Surfaces With Application to Supersonic-Tunnel Contour Correction. NACA TN 2045, 1950.

9. Ferri, Antonio: Elements of Aerodynamics of Supersonic Flows. The Macmillan Co., 1949.

10. Liepmann, H. W., Roshko, A., and Dhawan, S.: On Reflection of Shock Waves From Boundary Layers. NACA Rep. 1100, 1952. (Supersedes NACA TN 2334.)

TABLE I.- SOME QUANTITIES USED IN CALCULATING THE REQUIRED OPEN RATIO FOR THE TEST SECTION OF THE 3-INCH BY 3-INCH TRANSONIC TUNNEL

$[H_{o1} = 2{,}086.54$ lb/sq ft; $T_{o1} = 200^{\circ}$ F$]$

| $\delta_2$ | $M_2$ | $H_2/H_{o1}$ | $\rho_2$ | $V_2$ | $P_j$ | $P_j/H_{j2}$ | $M_{j2}$ | $\rho_{j2}$ | $V_{j2}$ | $m_{nb1}$ | $m_{nt2}$ | $V_2/V_j$ | $\sigma$ | r |
|---|---|---|---|---|---|---|---|---|---|---|---|---|---|---|
| 0 | 1.278 | 1.000 | 0.000909 | 1399.2 | 769.87 | 0.3690 | 1.284 | 0.000904 | 1403.8 | 0.008 | 0 | 0.9967 | 0.0134 | 47.0 |
| .32 | 1.266 | 1.000 | .0009187 | 1389.2 | 769.87 | .3690 | 1.284 | .000904 | 1403.8 | .008 | .01514 | .9896 | .0248 | 48.2 |
| 1.52 | 1.220 | 1.000 | .0009606 | 1350.4 | 769.87 | .3690 | 1.284 | .000904 | 1403.8 | .008 | .04241 | .9619 | .0635 | 52.7 |
| 2.57 | 1.177 | .9998 | .0009997 | 1313.3 | 769.87 | .3690 | 1.284 | .000904 | 1403.8 | .008 | .06687 | .9355 | .1120 | 47.1 |
| 3.49 | 1.136 | .9996 | .001037 | 1277.0 | 769.87 | .3691 | 1.283 | .000903 | 1403.6 | .008 | .08860 | .9098 | .1600 | 43.7 |
| 4.27 | 1.097 | .9991 | .001073 | 1242.0 | 769.87 | .3693 | 1.283 | .000903 | 1403.3 | .008 | .10726 | .8850 | .1950 | 43.4 |
| 4.93 | 1.061 | .9984 | .001107 | 1208.8 | 769.87 | .3696 | 1.282 | .000903 | 1402.8 | .008 | .12300 | .8617 | .2256 | 43.0 |

TABLE II.- TABULATION OF SOME VALUES USED TO FIND THE PLENUM-CHAMBER PRESSURE FOR A BOUNDARY-LAYER GROWTH RATE $m_{nbl}$ = 0.008 SLUG/FT$^2$-SEC AND FOR AN r = 0.47

| $P_j/H_{j1}$ | $P_j$ | $\rho_{j1}$ | $V_{j1}$ | $V_s/V_{j1}$ | $\sigma$ | $m_{nt}$ $(\rho_{j1}V_{j1}r\sigma)$ |
|---|---|---|---|---|---|---|
| 0.3694 | 770.82 | 0.000905 | 1403.1 | 0.9972 | 0.0127 | 0.00758 |
| .3690 | 769.87 | .000904 | 1403.8 | .9967 | .0134 | .00799 |
| .3685 | 768.82 | .000903 | 1404.6 | .9962 | .0142 | .00846 |
| .3656 | 762.82 | .000898 | 1409.3 | .9928 | .0200 | .01190 |

TABLE III.- SOME QUANTITIES USED IN CALCULATING THE REQUIRED OPEN RATIO FOR THE 3-INCH BY 3-INCH TEST SECTION WHEN USING THE ESTIMATED BOUNDARY-LAYER METHOD

$\left[H_{o1} = 2{,}086.54 \text{ lb/sq ft}; T_{o1} = 200^{\circ} \text{ F}\right]$

| $\delta_2$ | $M_2$ | $H_2/H_{o1}$ | $\rho_2$ | $V_2$ | $P_j$ | $P_j/H_{j2}$ | $M_{j2}$ | $\rho_{j2}$ | $V_{j2}$ | $V_{nt}/V_s$ | $d\delta^*/dx_p$ | $d\delta^*/dx_{sw}$ | $m_{nbl}$ | $m_{nt2}$ | $V_2/V_j$ | $\sigma$ | r |
|---|---|---|---|---|---|---|---|---|---|---|---|---|---|---|---|---|---|
| 0 | 1.278 | 1.000 | 0.000909 | 1399.2 | 771.9 | 0.3700 | 1.282 | 0.0009053 | 1402.1 | 0.0054 | 0.00345 | 0.002 | 0.00688 | 0.00688 | 0.9978 | 0.0115 | 47.0 |
| .32 | 1.266 | 1.000 | .0009197 | 1389.2 | 771.9 | .3700 | 1.282 | .0009053 | 1402.1 | .0091 | .00172 | .002 | .0047 | .01184 | .9908 | .0233 | 40.0 |
| 1.52 | 1.220 | 1.000 | .0009606 | 1350.4 | 771.9 | .3700 | 1.282 | .0009053 | 1402.1 | .0265 | .00026 | .002 | .00288 | .03729 | .9631 | .0624 | 47.1 |
| 2.57 | 1.177 | .9998 | .0009997 | 1313.3 | 771.9 | .3700 | 1.282 | .0009053 | 1402.1 | .0470 | 0 | .002 | .00257 | .06144 | .9367 | .1094 | 44.2 |
| 3.49 | 1.136 | .9996 | .001037 | 1277.6 | 771.9 | .3701 | 1.281 | .0009050 | 1402.1 | .0627 | 0 | .002 | .00260 | .08320 | .9108 | .1562 | 42.0 |
| 4.27 | 1.097 | .9991 | .001073 | 1242.0 | 771.9 | .3703 | 1.281 | .0009049 | 1402.1 | .0764 | 0 | .002 | .00261 | .10187 | .8861 | .1940 | 41.4 |
| 4.93 | 1.061 | .9984 | .001107 | 1208.8 | 771.9 | .3705 | 1.281 | .0009048 | 1402.0 | .0882 | 0 | .002 | .00262 | .11762 | .8626 | .2247 | 41.3 |

TABLE IV.- SOME QUANTITIES USED IN CALCULATING THE OPEN-RATIO DISTRIBUTION IN THE FLOW-GENERATION REGION OF A 3-INCH BY 3-INCH TRANSONIC TUNNEL

$\left[T_{ol} = 200^{\circ}\ F;\ H_{ol} = 2{,}086.54\ lb/sq\ ft;\ \rho_{jl} = 0.000904\ slug/cu\ ft;\ and\ V_{jl} = 1{,}403.8\ ft/sec\right]$

| Station | $\nu_a$ | $\nu_b$ | $\nu_s$ | $M_s$ | $V_s$ | $V_s/V_{jl}$ | $\dot{\sigma}$ | $m_{nbl}$ | $m_{ex}$ $(\rho_s V_s \sin \delta)$ | $m_{nt}$ | r, percent |
|---|---|---|---|---|---|---|---|---|---|---|---|
| 0 | 0 | 0 | 0 | 1.0000 | 1151.2 | 0.8200 | 0.2790 | 0 | 0 | 0 | 0 |
| .2 | .372 | .013 | .385 | 1.0425 | 1191.5 | .8487 | .2430 | .00107 | .00841 | .00948 | 3.07 |
| .4 | .744 | .030 | .774 | 1.0684 | 1215.6 | .8659 | .2200 | .00212 | .01669 | .01881 | 6.74 |
| .6 | 1.117 | .058 | 1.175 | 1.0913 | 1236.8 | .8810 | .2010 | .00318 | .02471 | .02789 | 10.93 |
| .8 | 1.489 | .098 | 1.587 | 1.1127 | 1256.1 | .8948 | .1825 | .00424 | .03233 | .03657 | 15.79 |
| 1.0 | 1.860 | .170 | 2.030 | 1.1341 | 1275.4 | .9085 | .1620 | .00530 | .03912 | .04442 | 21.61 |
| 1.2 | 2.233 | .269 | 2.502 | 1.1553 | 1294.3 | .9220 | .1370 | .00638 | .04524 | .05162 | 29.68 |
| 1.3 | 2.420 | .329 | 2.749 | 1.1680 | 1303.7 | .9287 | .1245 | .00690 | .04805 | .05495 | 34.78 |
| 1.4 | 2.606 | .398 | 3.004 | 1.1771 | 1313.4 | .9356 | .1110 | .00743 | .05061 | .05804 | 41.19 |
| 1.5 | 2.790 | .470 | 3.260 | 1.1882 | 1323.2 | .9426 | .0985 | .00800 | .05303 | .06103 | 48.82 |
| 1.6 | 2.790 | .548 | 3.338 | 1.1912 | 1325.8 | .9444 | .0950 | .00800 | .05119 | .05919 | 49.08 |
| 1.7 | 2.790 | .628 | 3.418 | 1.1944 | 1328.5 | .9463 | .0910 | .00800 | .04931 | .05731 | 49.62 |
| 1.8 | 2.790 | .713 | 3.503 | 1.1977 | 1331.4 | .9484 | .0880 | .00800 | .04733 | .05533 | 49.53 |
| 1.9 | 2.790 | .800 | 3.590 | 1.2014 | 1334.5 | .9506 | .0840 | .00800 | .04533 | .05333 | 50.03 |
| 2.0 | 2.790 | .892 | 3.682 | 1.2052 | 1337.8 | .9530 | .0800 | .00800 | .04316 | .05116 | 50.40 |
| 2.2 | 2.790 | 1.081 | 3.871 | 1.2125 | 1344.1 | .9575 | .0720 | .00800 | .03880 | .04680 | 51.20 |
| 2.4 | 2.790 | 1.275 | 4.065 | 1.2202 | 1350.5 | .9620 | .0640 | .00800 | .03431 | .04231 | 52.11 |
| 2.6 | 2.790 | 1.480 | 4.270 | 1.2285 | 1357.7 | .9671 | .0565 | .00800 | .02958 | .03758 | 54.41 |
| 2.8 | 2.790 | 1.690 | 4.480 | 1.2366 | 1364.6 | .9721 | .0495 | .00800 | .02479 | .03279 | 52.21 |
| 3.0 | 2.790 | 1.900 | 4.690 | 1.2448 | 1371.5 | .9770 | .0430 | .00800 | .02000 | .02880 | 51.28 |
| 3.2 | 2.790 | 2.120 | 4.910 | 1.2532 | 1378.5 | .9820 | .0362 | .00800 | .01500 | .02300 | 50.11 |
| 3.4 | 2.790 | 2.342 | 5.132 | 1.2615 | 1385.5 | .9869 | .0296 | .00800 | .01001 | .01801 | 47.90 |
| 3.6 | 2.790 | 2.570 | 5.360 | 1.2699 | 1392.4 | .9919 | .0214 | .00800 | .00490 | .01290 | 47.43 |
| 3.79 | 2.790 | 2.790 | 5.580 | 1.2780 | 1399.2 | .9967 | .0134 | .00800 | 0 | .00800 | 47.03 |

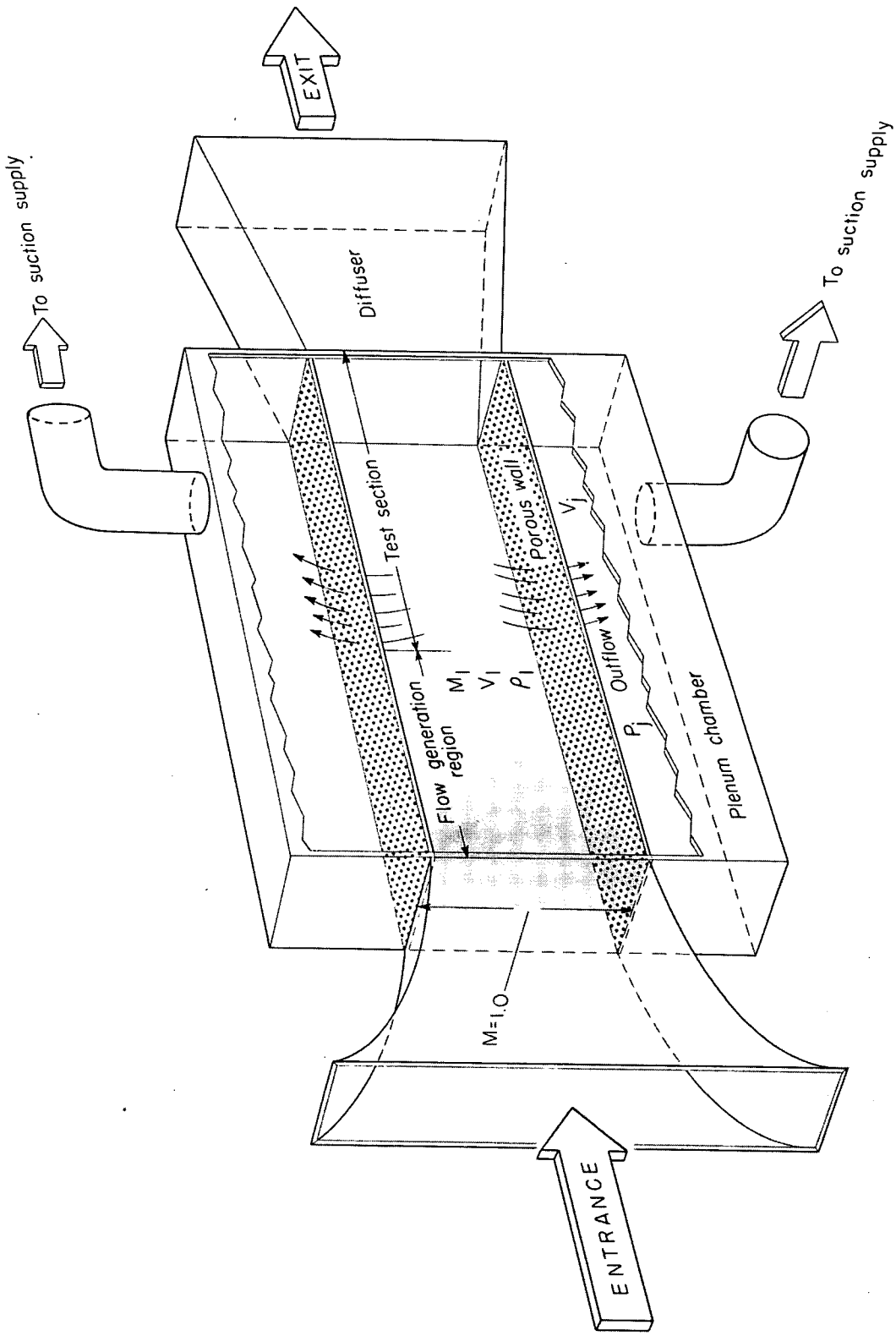


L-90524

Figure 1.- A schematic drawing showing how air enters and leaves a porous-wall wind tunnel designed by the general design method.

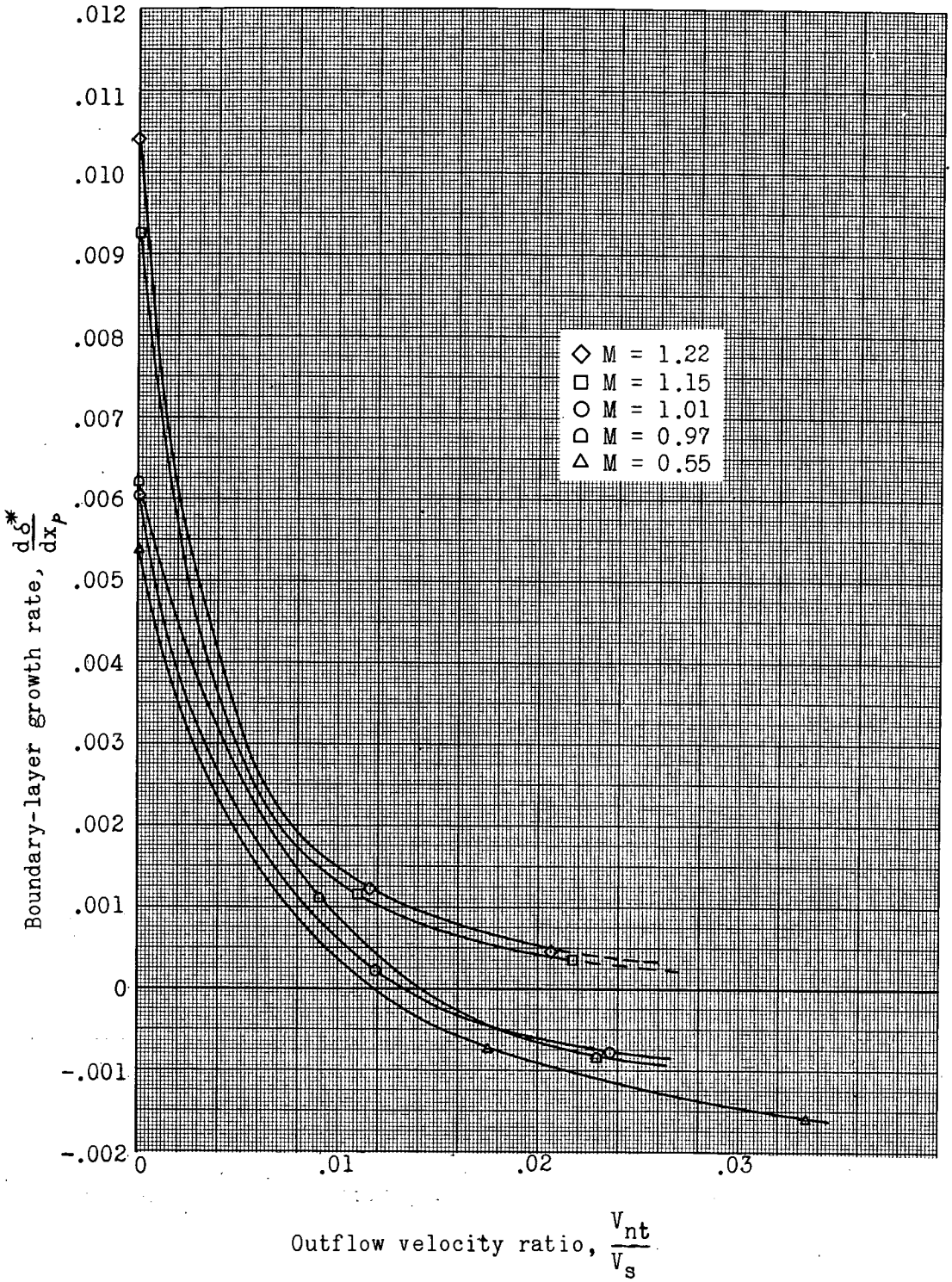


Figure 2.- Curves showing how $d\delta^*/dx_p$ varies with the outflow velocity ratio for several Mach numbers over a 41-percent-open perforated specimen.

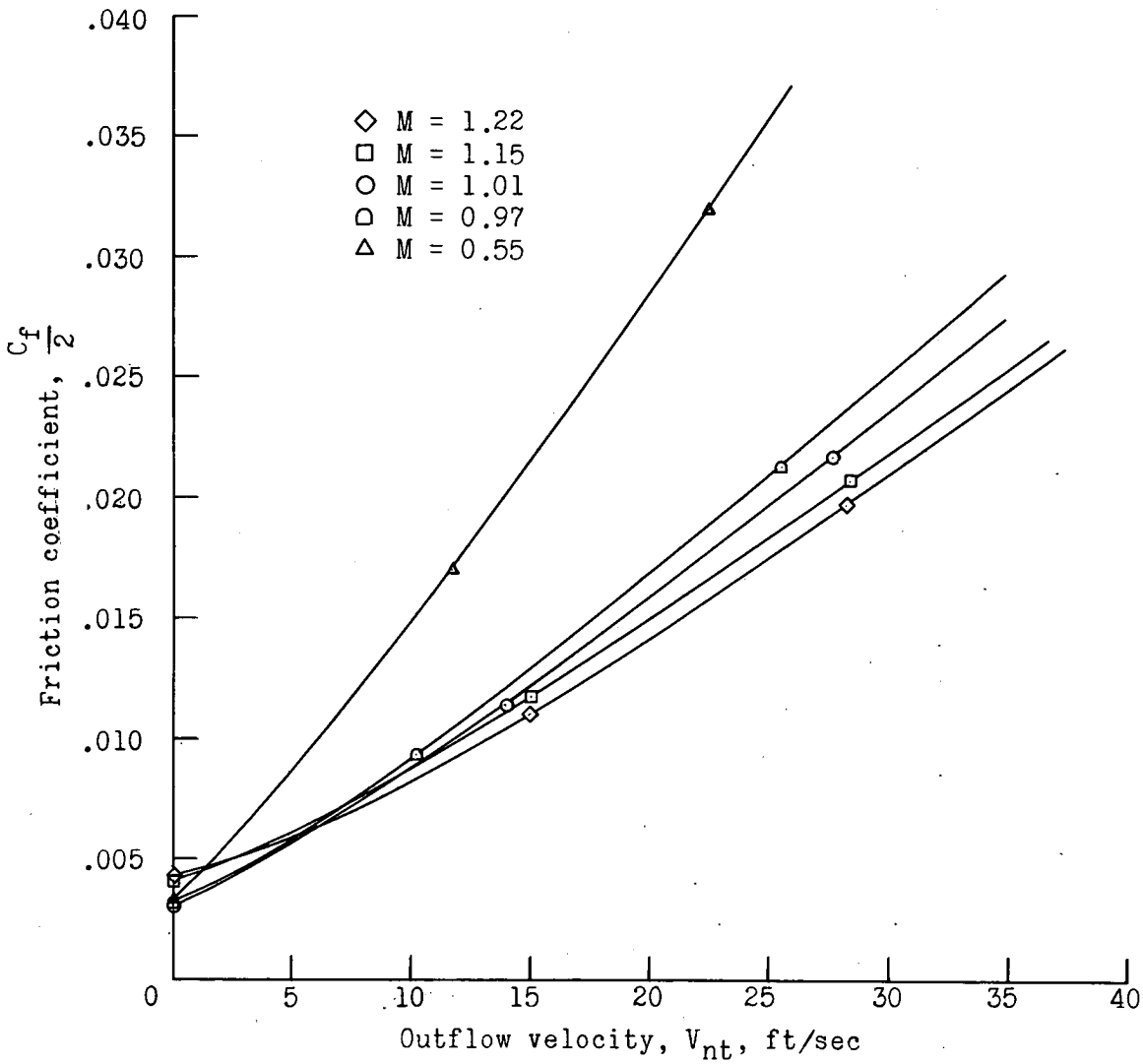


Figure 3.- Curves describing how the friction coefficient varies with outflow velocity for a 41-percent-open perforated specimen.

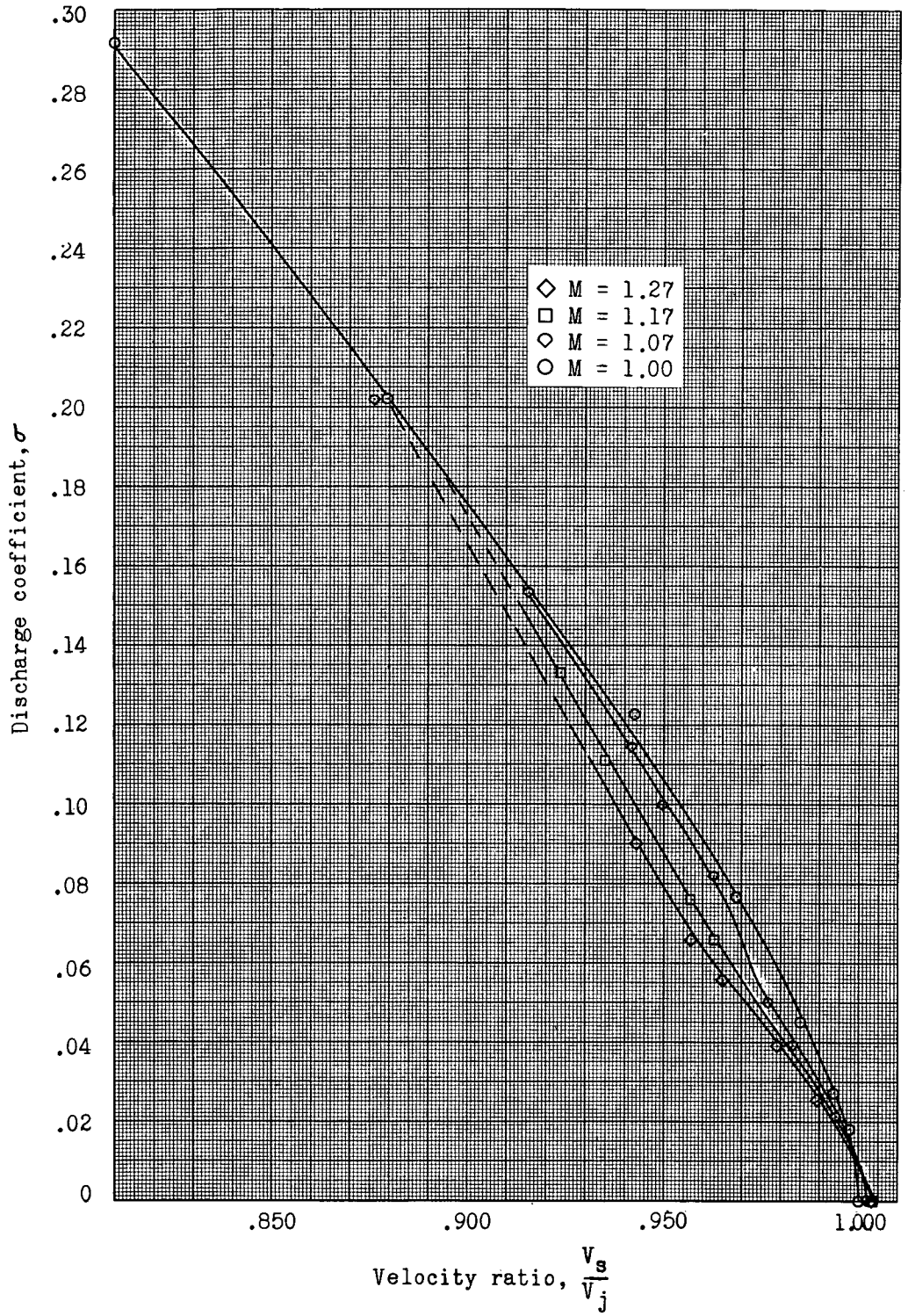


Figure 4.- Discharge coefficients for a 41-percent-open perforated specimen having an incoming boundary-layer displacement thickness of approximately 0.002 inch.

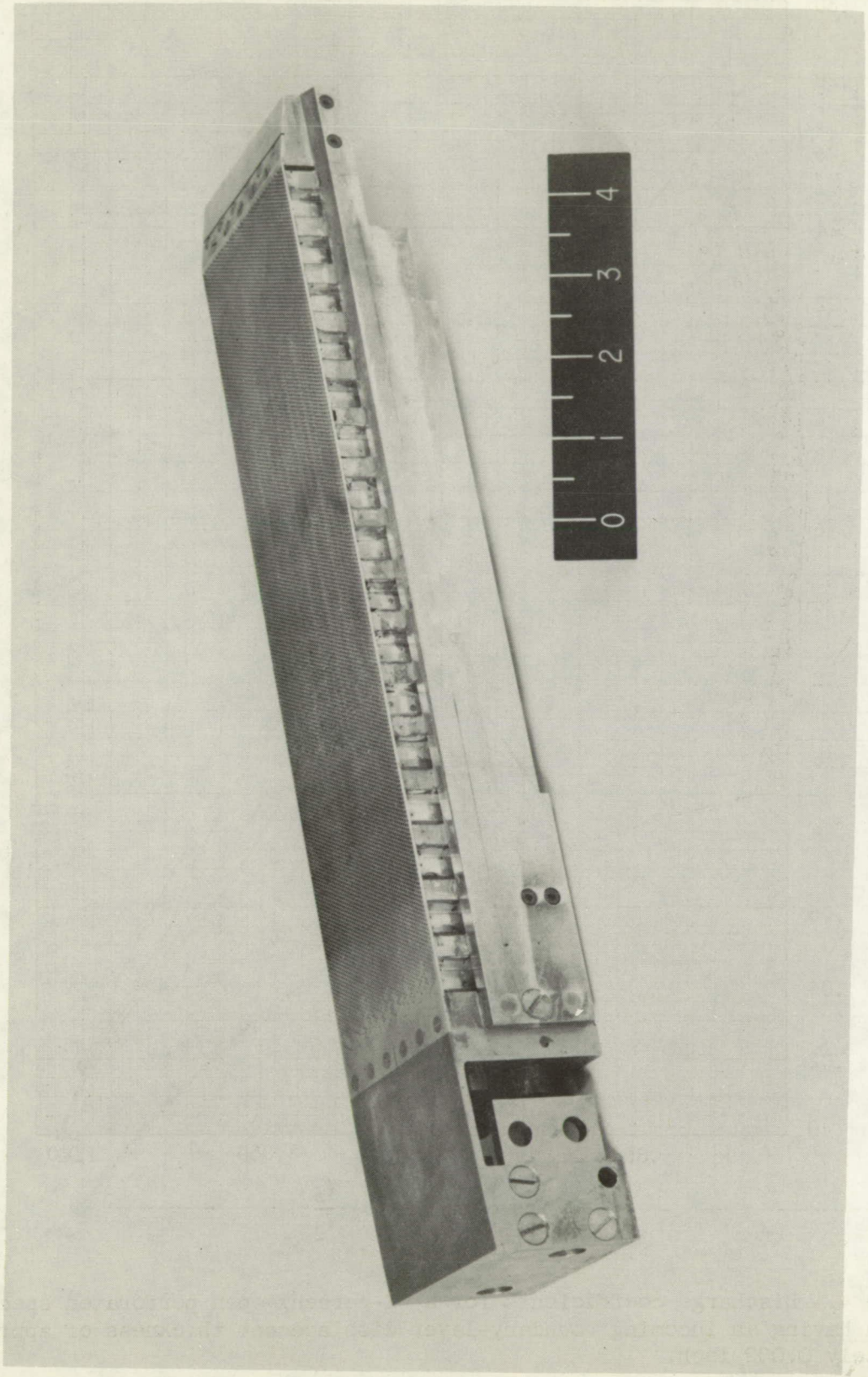


L-89921

Figure 5.- Picture of the perforated wall used for experimentally examining the effectiveness of the design method.

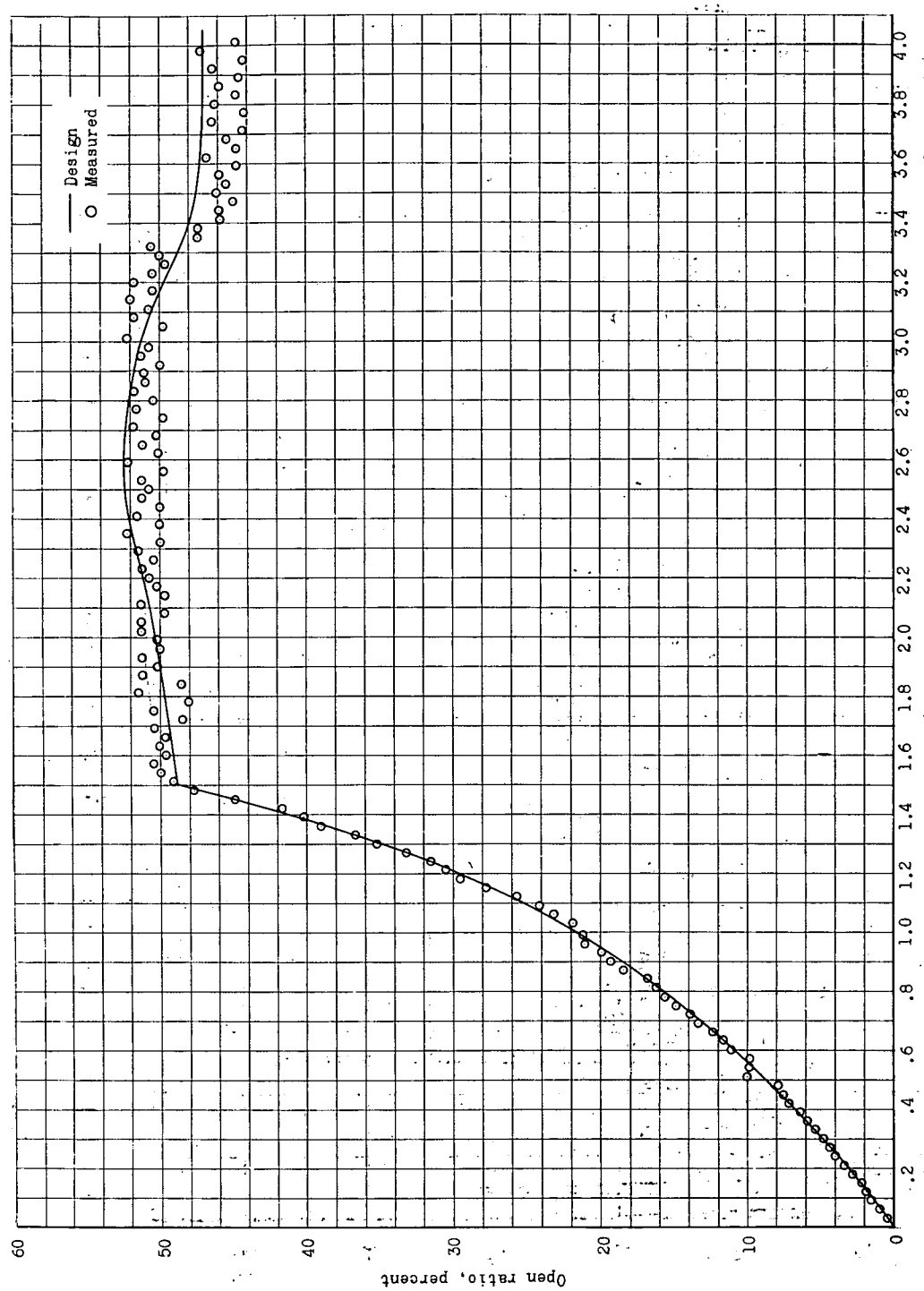


Figure 6.- Data showing the differences between the design open ratio and that achieved in construction.

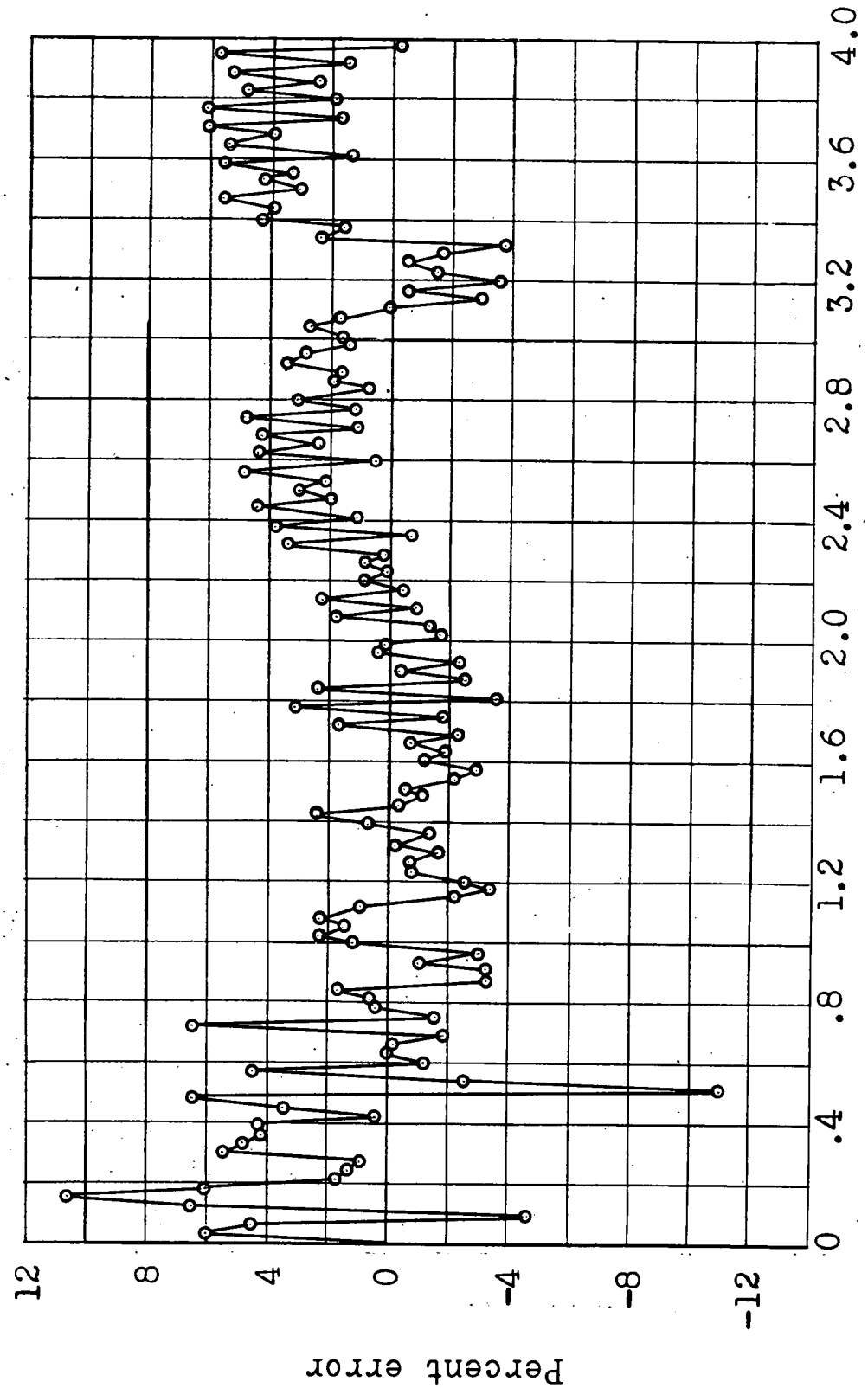


Figure 7.- Points indicating the percent error between the design open ratio and that obtained by construction.

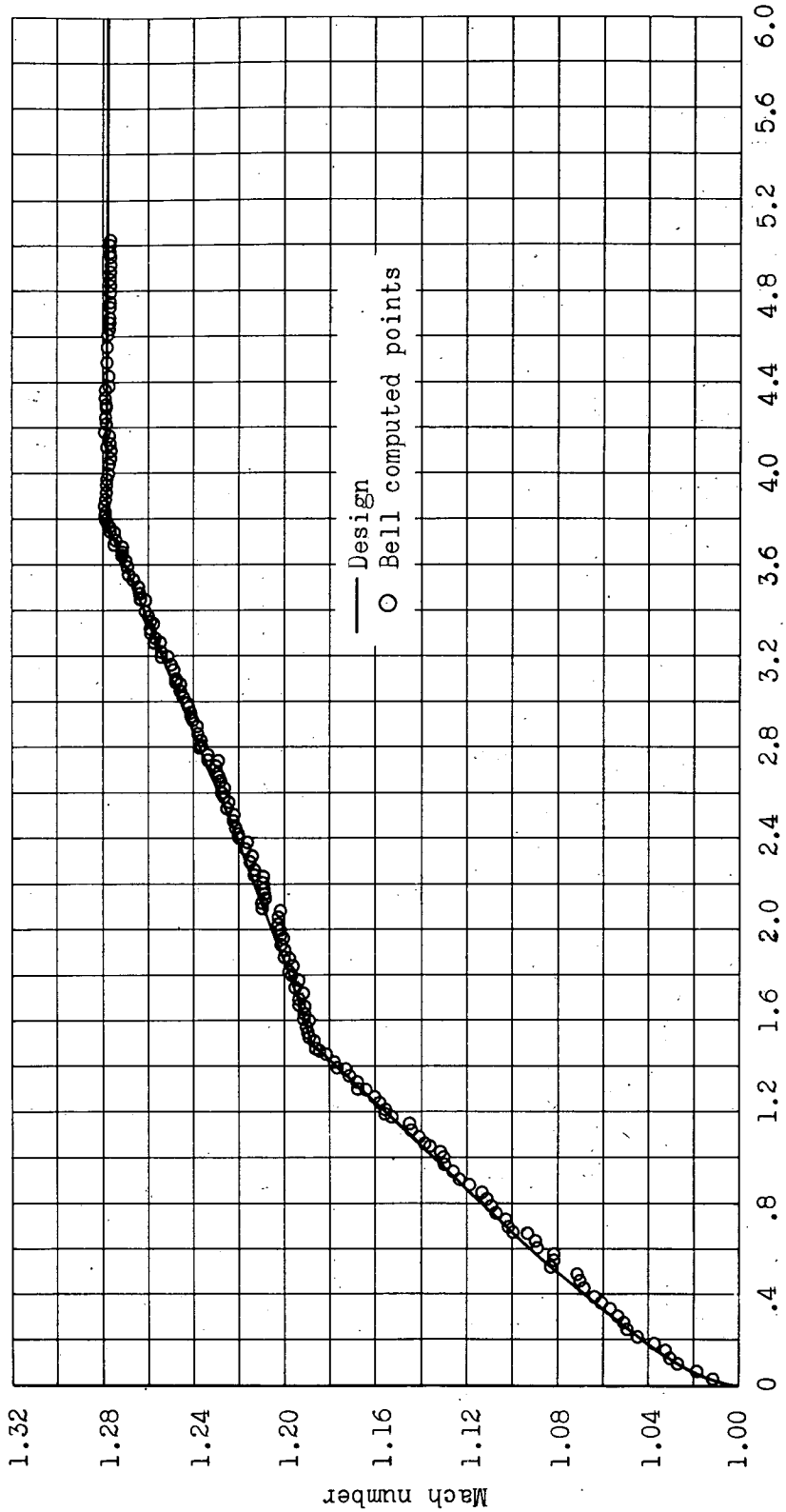


(a) Distribution along tunnel porous walls.

Figure 8.- Calculated and design Mach number distributions for a 3- by 3-inch tunnel.

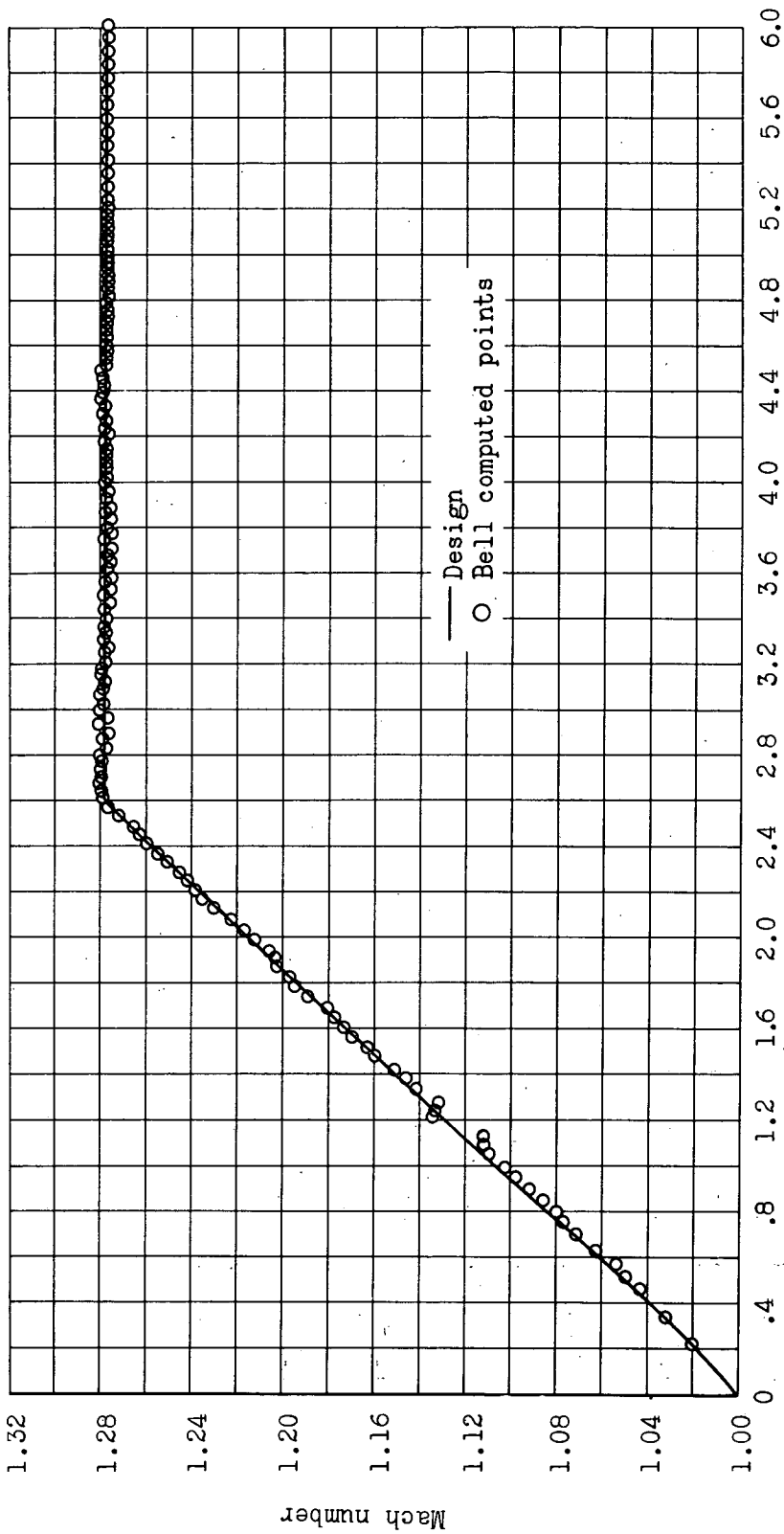


(b) Distribution along tunnel center line.

Figure 8.- Concluded.

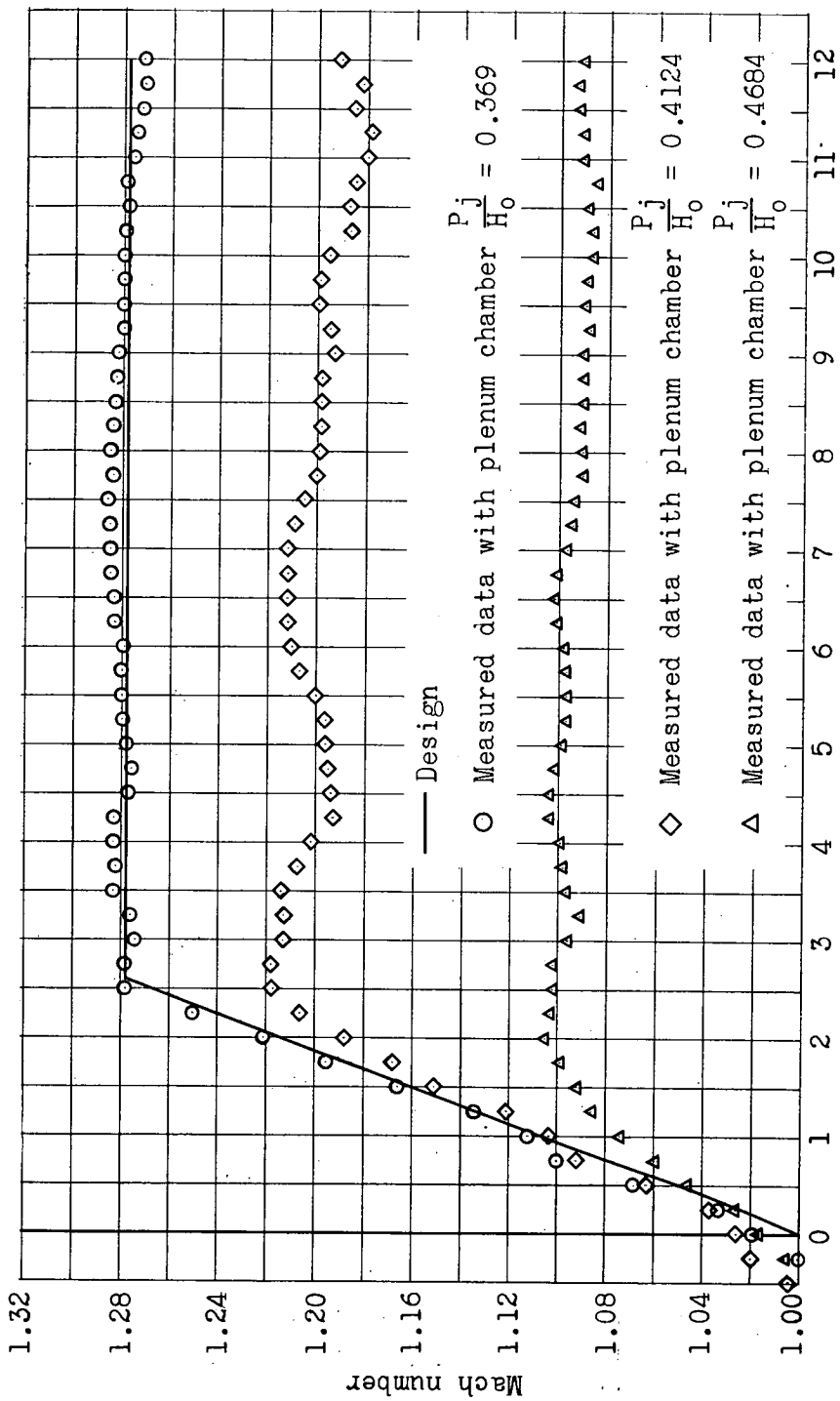


Figure 9.- Relationship between the tunnel design Mach number distributions and those obtained experimentally.